

Beyond Rigid: Benchmarking Non-Rigid Video Editing

Bingzheng Qu¹, Kehai Chen^{1*}, Xuefeng Bai¹, Jun Yu², Min Zhang¹

¹Institute of Computing and Intelligence, Harbin Institute of Technology, Shenzhen, China

²School of Intelligence Science and Engineering, Harbin Institute of Technology, Shenzhen, China

qbzz@stu.hit.edu.cn, chenkehai@hit.edu.cn

Abstract

Despite the remarkable progress in text-driven video editing, generating coherent non-rigid deformations remains a critical challenge, often plagued by physical distortion and temporal flicker. To bridge this gap, we propose NRVBench, the first dedicated and comprehensive benchmark designed to evaluate non-rigid video editing. First, we curate a high-quality dataset consisting of 180 non-rigid motion videos from six physics-based categories, equipped with 2,340 fine-grained task instructions and 360 multiple-choice questions. Second, we propose NRVE-Acc, a novel evaluation metric based on Vision-Language Models that can rigorously assess physical compliance, temporal consistency, and instruction alignment, overcoming the limitations of general metrics in capturing complex dynamics. Third, we introduce a training-free baseline, VM-Edit, which utilizes a dual-region denoising mechanism to achieve structure-aware control, balancing structural preservation and dynamic deformation. Extensive experiments demonstrate that while current methods have shortcomings in maintaining physical plausibility, our method achieves excellent performance across both standard and proposed metrics. We believe the benchmark could serve as a standard testing platform for advancing physics-aware video editing.

1 Introduction

With the rapid development of text-to-image and text-to-video generative models [Blattmann *et al.*, 2023; Ma *et al.*, 2025; Team Wan *et al.*, 2025; Rombach *et al.*, 2022; Feng *et al.*, 2025], generative video editing has emerged as an active research direction, yielding a large number of text-driven editing approaches. Consequently, evaluation standards are evolving. The focus is moving beyond simple appearance changes to prioritize motion controllability and temporal consistency.

*Corresponding author.

However, non-rigid editing remains a critical bottleneck. Yoon *et al.* [Yoon *et al.*, 2024] highlight a significant gap, noting that while existing methods excel at rigid-type editing like appearance changes, they face severe limitations in non-rigid motion scenarios, particularly for tuning-free methods. This inherent difficulty in managing complex motion is further corroborated by recent studies [Zhong *et al.*, 2024; Koo *et al.*, 2024; Chang *et al.*, 2025], which report persistent physical inconsistencies and temporal flickering. Exacerbating this challenge is the scarcity of suitable benchmarks. Representative datasets like TGVE [Wu *et al.*, 2023b] and TGVE+ [Singer *et al.*, 2024] primarily focus on general editing tasks, failing to capture the physical intricacies. While the recent FiVE benchmark [Li *et al.*, 2025] includes non-rigid deformation as a key category in its fine-grained classification, it lacks targeted evaluation protocols to verify physical adherence. This makes it difficult to assess whether edited videos maintain deformation realism, physical plausibility, and fine temporal consistency, thereby restricting fair comparisons and systematic progress in non-rigid video editing.

To empirically validate this gap and guide the design of a principled evaluation framework, we first conduct a preliminary study with a pilot benchmark, denoted as **Benchmark-V0**. We curated 15 representative videos exhibiting diverse non-rigid motion, categorized into three distinct regimes: Articulated, Fluid, and Elastoplastic. To ensure granular assessment, we designed a hierarchical instruction set covering 9 fine-grained editing types across three difficulty levels. This yields a test suite of 225 edit instructions, each paired with a pixel-accurate mask. As shown in Table 2, results under commonly used metrics reveal substantial performance limitations in non-rigid editing scenarios. Beyond confirming the intrinsic difficulty of non-rigid deformation, Benchmark-V0 provides actionable guidance for calibrating task difficulty, which we leverage to scale up to our full benchmark.

Motivated by these findings and the demand for standardized evaluation, we propose **NRVBench** (**N**on-**R**igid **V**ideo **E**ditioning **B**enchmark), a dedicated evaluation suite designed to rigorously assess non-rigid editing capabilities. NRVBench features 180 carefully curated videos spanning six physics-grounded categories, enriched with 2,340 fine-grained edit instructions, 360 MCQs, and corresponding

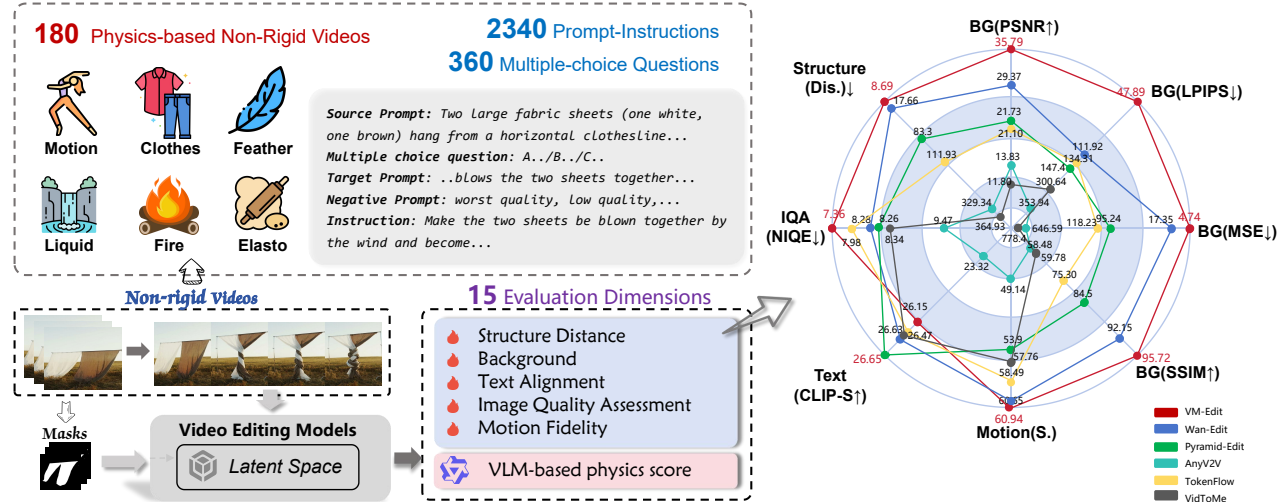


Figure 1: Overview of **NRVBench**. The left side is the framework of NRVBench, which contains 180 physics-based non-rigid motion videos across six categories, paired with 2,340 fine-grained editing instructions and 360 multiple-choice questions. The right side is the traditional metrics results of six video editing models.

pixel-accurate masks, which support both comprehensive benchmarking and targeted diagnosis. To ensure reliable assessment, we accompany this benchmark with **NRVE-Acc** (Non-Rigid Video Editing Adherence score), a VLM-based metric that jointly evaluates three critical dimensions: instruction alignment, physics plausibility, and temporal consistency. Specifically, NRVE-Acc queries a VLM judge with category-conditioned questions and optical-flow visualization, providing a faithful indicator of editing success by assessing physical plausibility through motion cues. Finally, in order to establish a robust baseline, we also propose VM-Edit, as illustrated in Figure 3, a training-free baseline that obviates the need for manual motion guidance. Specifically, VM-Edit employs a mask-guided dual-region denoising strategy. By applying a multi-stage editing mode within the masked area, it enables precise non-rigid editing while strictly preserving the original background consistency.

We conduct a comprehensive evaluation of five representative video editing methods alongside our baseline, VM-Edit, on both the pilot benchmark and NRVBench. Our results reveal that existing approaches exhibit significant limitations in handling non-rigid motion. Furthermore, our analysis demonstrates that NRVE-Acc provides a more physics-aware evaluation than traditional metrics. Finally, VM-Edit establishes a robust baseline for this challenging task, showing promising capabilities in addressing the complexities of non-rigid video editing tasks. Our contributions are summarized as follows:

- We present **NRVBench**, the first comprehensive benchmark tailored for **non-rigid video editing**. It features 180 physics-grounded videos across six categories, equipped with 2,340 fine-grained edit instructions, 360 multiple-choice questions (MCQs), and pixel-accurate masks to enable rigorous evaluation.

- We devise **NRVE-Acc**, a VLM-based metric that evaluates physics-aware deformation plausibility for non-rigid video editing methods.
- We develop **VM-Edit**, a training-free, structure-aware baseline with a dual-region denoising mechanism for precise region-conditioned editing. By effectively balancing foreground plasticity with background stability, it establishes a robust baseline for the challenging task of non-rigid video editing.

2 Related Work

2.1 Video Editing Benchmark and metrics

Several benchmarks have emerged to systematize controllable video editing evaluation. While benchmarks like TGVE [Wu *et al.*, 2023b], FiVE [Li *et al.*, 2025], and V2VBench [Sun *et al.*, 2024] have established standardized protocols for video editing methods, they exhibit a clear limitation: a lack of focus on non-rigid motion. Existing evaluations primarily prioritize visual style or semantic alignment, failing to verify whether deformations adhere to physical laws. This limitation is mirrored in standard metrics like CLIP [Wu *et al.*, 2021] and LPIPS [Zhang *et al.*, 2018]. Predicated on strict spatial or semantic correspondence, these metrics often misclassify plausible non-rigid motion as artifacts, while conversely failing to penalize physically incoherent distortions. Motivated by this gap, we introduce **NRVBench** and **NRVE-Acc** to support physics-aware evaluation of **non-rigid video editing**, filling a missing dimension in existing benchmarks and metrics that are primarily designed for generic or appearance-level edits.

2.2 Video Editing Methods

Recent advancements in video editing can be broadly categorized into training-free [Zhu *et al.*, 2025; Qi *et*

Benchmark	#Videos	Video Source	#Prompts	T-step	Src. Mask	Phys.-aware	Taxonomy
BalanceCC [Feng <i>et al.</i> , 2024]	100	–	400	✗	✗	✗	Task-level
V2VBench [Sun <i>et al.</i> , 2024]	50	Internet	150	✗	✗	✗	Task-level
TGVE [Wu <i>et al.</i> , 2023b]	76	DAVIS, YouTube, Videvo	304	✗	✗	✗	Task-level
TGVE+ [Singer <i>et al.</i> , 2024]	76	DAVIS, YouTube, Videvo	1417	✗	✗	✗	Task-level
FiVE [Li <i>et al.</i> , 2025]	100	DAVIS + Gen.	420	✗	✓	✗	Object-level
VEditBench [Wu <i>et al.</i> , 2025]	420	YouTube, Videvo	2520	✗	✗	✗	Task-level
NRVBench (Ours)	180	DAVIS, Pexels	2340	✓	✓	✓	Physics-level

Table 1: Comparison of controllable video editing benchmarks and metrics.

al., 2023; Wang *et al.*, 2024; Yang *et al.*, 2025] and training-based paradigms [Tu *et al.*, 2025; Ouyang *et al.*, 2024; Mou *et al.*, 2024; Deng *et al.*, 2024]. Despite their success in rigid editing, both paradigms face critical bottlenecks when confronting non-rigid content. Methods like TokenFlow [Geyer *et al.*, 2024] and Rerender-A-Video [Yang *et al.*, 2023] rely on inter-frame correspondences to align generated content. While effective in static scenes, this strategy struggles to handle non-rigid scenarios like fluid flow, where correspondence maps are often discontinuous. Similarly, propagation-based approaches like AnyV2V [Ku *et al.*, 2024] provide insufficient temporal guidance, leading to temporal inconsistency during large deformations. Conversely, training-based methods such as Tune-A-Video [Wu *et al.*, 2023a] and MotionEditor [Tu *et al.*, 2024] fine-tune the model on the source video. While this improves fidelity, it frequently results in overfitting to the original rigid structures, restricting the model’s ability to generate new, dynamic motion patterns. Similarly, recent concurrent work such as DNI [Yoon *et al.*, 2024] and ByteMorph [Chang *et al.*, 2025] argue that current diffusion paradigms contain an inherent bias toward rigid transformations, leaving the domain of non-rigid motion largely unaddressed. Collectively, these studies substantiate that robust non-rigid video editing, particularly when confronting large or discontinuous deformations, constitutes a critical and widely acknowledged bottleneck at the current frontier. To facilitate future research, we propose VM-Edit. Diverging from previous global optimization methods, our training-free approach adopts a region-conditioned strategy. This enables precise non-rigid motion editing in the foreground while rigorously preserving background stability.

3 NRVBench and NRVE-Acc

In this section, we introduce NRVBench, a comprehensive video editing benchmark spanning six non-rigid target categories, as shown in Figure 1. Complementing this benchmark, we further propose NRVE-Acc, a physics-grounded metric that evaluates editing correctness via VLM-based structured QA.

3.1 NRVBench

Pilot Benchmark. Benchmark-V0 serves as our preliminary benchmark, comprising 15 representative videos across three target categories to ensure broad coverage of common non-rigid motions. To facilitate granular assessment, we

introduce a hierarchical difficulty taxonomy that categorizes edits into three levels based on physical constraints:

- **Level-1 (Degree Editing):** Involves continuous deformation that preserves the underlying topology (e.g., modifying deformation magnitude).
- **Level-2 (Topology Editing):** Entails structural changes that alter connectivity or geometry, such as splitting, merging, or contact-driven deformations.
- **Level-3 (Attribute Editing):** Modifies intrinsic material or dynamic properties (e.g., stiffness, viscosity), requiring the generation of physically consistent appearance and motion patterns.

We evaluated multiple representative baselines on a pilot benchmark to comprehensively analyze prompt difficulty and model performance. The preliminary assessment revealed a general decline in indicators in the current model, especially in cases of large deformations, topological changes, or attribute changes. These insights were used to calibrate the difficulty range and instance composition of our final NRVBench. The quantitative results of this pilot study are reported in Table 2.

Video Dataset Construction. Expanding upon the insights from Benchmark-V0, we significantly scale up our benchmark to NRVBench, comprising 180 high-quality non-rigid motion videos curated from the DAVIS dataset [Perazzi *et al.*, 2016] and Pexels*. To ensure standardized evaluation under model constraints, each video is trimmed to 60 frames for the model’s editing. For textual annotation, we employ GPT-4o [OpenAI *et al.*, 2024] to generate structured captions based on frames uniformly sampled at 15-frame intervals. Furthermore, we generate segmentation masks using SAM2 [Ravi *et al.*, 2024], followed by rigorous human verification and correction. We provide a detailed comparison with existing models in Table 1.

Six Non-Rigid Target Categories. To cover diverse editing regimes, we taxonomize our benchmark into six categories based on physical properties:

- **ASB** (Articulated Soft Bodies): Targets anatomical consistency and joint constraints in humans and animals.
- **CTS** (Cloth and Thin-Shells): Focuses on surface continuity and folding dynamics in fabrics.

*<https://www.pexels.com/license/>

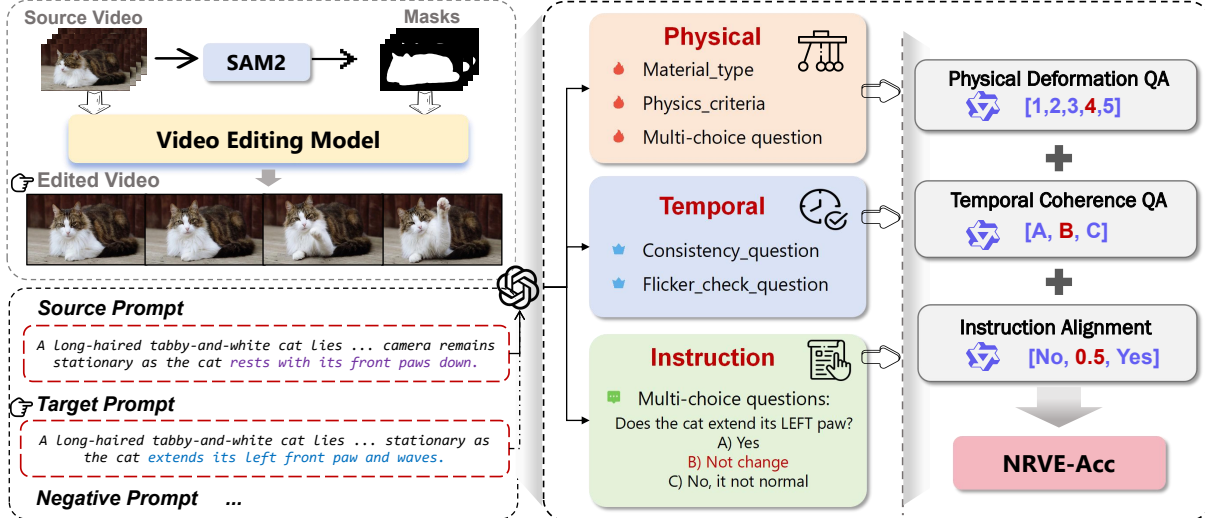


Figure 2: **Overview of the NRVE-Acc Evaluation Pipeline.** Our framework utilizes standardized source/target prompt pairs to guide the editing models. We use GPT-4o to generate detailed annotations. The generated videos are then evaluated by Qwen2.5-VL using a hierarchical Question-Answer(QA) mechanism, focusing on (a) Instruction Following, (b) Temporal Consistency, and (c) Material-Specific Deformation.

- **HFF** (Hair, Fur, and Feathers): Addresses strand coherence in fine, fibrous structures.
- **LFS** (Liquid Free Surfaces): Enforces volume conservation and flow fluidity.
- **GSF** (Gas, Smoke, and Fire): Models turbulence coherence and topological evolution.
- **DSO** (Deformable Solid Objects): Validates elastic recovery and general shape integrity.

This structured taxonomy enables our metric to conduct targeted, category-specific inquiries.

Instruction and QA Construction. Leveraging the taxonomy from our pilot study, we utilized GPT-4o to synthesize 2,340 template-driven editing instructions spanning various complexities. To ensure precise evaluation, we further constructed 360 discriminating MCQs tailored for VLM-based judgment. Crucially, each video is assigned two deformation indices that controls the editing schedule by switching the model among three editing states, keeping the requested edits within the permissible strength of the corresponding material regime. Each benchmark instance comprises aligned source/target prompts, object masks, ground-truth QA pairs, timesteps index, and negative prompts, facilitating a holistic evaluation of instruction following, physical plausibility, and temporal coherence.

3.2 NRVE-Acc

To address the challenges in evaluating non-rigid edits, we propose NRVE-Acc, a fine-grained metric designed to quantify both semantic instruction following and physics-consistent deformation. As illustrated in Figure 2, we leverage Qwen2.5-VL-7B as the visual-language judge. We query the judge independently for each evaluation dimension. Based on the sampled video representations (denoted by

V_{edit} for brevity), the judge produces three dimension scores $S_k(V_{\text{edit}})$ with $k \in \{\text{instr}, \text{phy}, \text{temp}\}$, corresponding to instruction faithfulness, physical plausibility, and temporal consistency, respectively.

Instruction Alignment Score (S_{instr}). This metric evaluates whether the edited content strictly adheres to the textual instruction. We employ a diagnostic MCQs derived from the target prompt. The VLM’s predicted option is matched against the ground truth, yielding a scalar score $S_{\text{instr}} \in [0, 1]$ based on prediction correctness.

Physics & Deformation Score (S_{phy}). We assess physical plausibility by conditioning the evaluation on the specific material category (e.g., LFS vs. DSO) defined in our benchmark. The VLM is prompted with category-specific physical plausibility criteria to rate visual realism on a Likert scale of 1 to 5. This rating is linearly normalized to the unit interval to derive the final score $S_{\text{phy}}(V_{\text{edit}})$.

Temporal Consistency Score (S_{temp}). To explicitly capture motion anomalies that may be subtle in pixel space, we leverage optical-flow visualization. Specifically, we construct flow maps from sampled frame triplets to highlight motion boundaries and continuity. The judge evaluates these flow visualizations for flickering or unnatural discontinuities, outputting a categorical verdict $\{A, B, C\} \mapsto \{100, 50, 0\}$ that is mapped to a scalar score $S_{\text{temp}}(V_{\text{edit}})$.

Final aggregation. For readability, we linearly map S_{instr} and S_{phy} to a 0–100 scale, and NRVE-Acc is computed from Eq. 1. Let $\mathcal{K} = \{\text{instr}, \text{phy}, \text{temp}\}$ and write $S_k = S_k(V_{\text{edit}})$ for brevity. We combine the three dimension scores using a weighted geometric mean:

$$\text{NRVE-Acc}(V_{\text{edit}}) = \prod_{k \in \mathcal{K}} (S_k + \epsilon)^{w_k}. \quad (1)$$

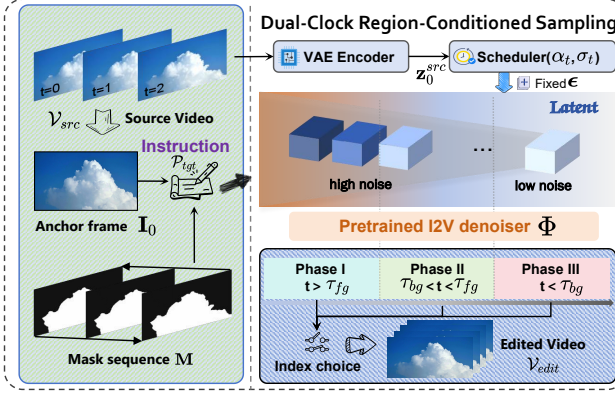


Figure 3: Overview of the VM-Edit model.

where we use uniform preset weights ($w_k = 1/3$) and $\epsilon = 10^{-6}$ for numerical stability. This aggregation acts as an adherence score that penalizes low performance in any single dimension, so achieving a high NRVE-Acc requires correct instruction following and physically plausible, temporally coherent non-rigid motion. The complete optical-flow computation, frame triplet selection, judge prompts, evaluation templates, sampling protocol, MCQs construction, and output-to-score parsing rules are provided in the supplementary materials.

4 VM-Edit

Inspired by region-conditioned diffusion sampling for controllable synthesis and editing, including TTM [Singer *et al.*, 2025], Blended Diffusion [Avrahami *et al.*, 2022], and RePaint [Lugmayr *et al.*, 2022], we identify region-wise sampling principle as a promising way to resolve the stability-plasticity dilemma in non-rigid video editing. Specifically, we propose VM-Edit (Figure 3), a structure-aware editing baseline that replaces manual motion guidance with an automated, region-conditioned pipeline. Designed to resolve the stability-plasticity dilemma, VM-Edit employs a region-conditioned sampling pipeline that dynamically allocates freedom to the foreground while locking the background, effectively eliminating temporal artifacts.

Problem Formulation. We formulate non-rigid video editing as synthesizing an edited video sequence \mathcal{V}_{edit} conditioned on a source video $\mathcal{V}_{src} = \{\mathbf{I}_i^{src}\}_{i=0}^{T-1}$ and a target textual instruction \mathcal{P}_{tgt} . VM-Edit is built on a pre-trained Image-to-Video (I2V) diffusion transformer (Wan2.2 [Team Wan *et al.*, 2025]) and operates in a strictly training-free manner by modifying only the sampling procedure. Inference takes four standardized inputs: (1) an Appearance Anchor $\mathbf{I}_0 = \mathbf{I}_0^{src}$ (the first frame) to preserve lighting/texture; (2) the Target Instruction \mathcal{P}_{tgt} specifying the desired non-rigid edit; (3) the Source Prior \mathcal{V}_{src} , which is encoded into a latent reference trajectory and injected via region-wise anchoring to provide motion and structure; and (4) a Spatial Layout mask sequence \mathbf{M} . We detail the mask details, systematic guide, and permissible editing strength in the appendices *C*.

Latent Reference Construction. Let $\text{Enc}(\cdot)$ be the pre-trained video VAE encoder of the I2V backbone, producing a latent video tensor \mathbf{z}_0 . We encode the source video to obtain a source-consistent reference by applying the encoder to the source video, i.e., $\mathbf{z}_0^{src} = \text{Enc}(\mathcal{V}_{src})$. To anchor regions at a matched noise level during sampling, we construct a noised source reference at each diffusion step t using the same noise schedule as the backbone:

$$\mathbf{z}_t^{src} = \alpha_t \mathbf{z}_0^{src} + \sigma_t \epsilon, \quad \epsilon \sim \mathcal{N}(0, \mathbf{I}), \quad (2)$$

where (α_t, σ_t) follow the model’s scheduler and ϵ is a standard Gaussian noise tensor with the same shape as \mathbf{z}_0^{src} , sampled once per video and reused for all t . For reproducibility, we sample ϵ once per video and reuse it across timesteps to obtain a consistent reference trajectory across noise levels.

Dual-Clock Region-Conditioned Sampling. Let \mathbf{z}_t denote the current latent at reverse diffusion step t (larger t indicates higher noise). Let $\Phi(\cdot)$ be one reverse-step update of the pre-trained denoiser/sampler, conditioned on \mathcal{P}_{tgt} and the anchor frame \mathbf{I}_0 :

$$\hat{\mathbf{z}}_{t-1} = \Phi(\mathbf{z}_t, t, \mathcal{P}_{tgt}, \mathbf{I}_0). \quad (3)$$

We enforce region-wise control by recomposing the next latent with a *foreground edit* term and a *background stabilization* term:

$$\mathbf{z}_{t-1} \leftarrow \mathbf{m} \odot \mathbf{z}_{t-1}^{fg} + (1 - \mathbf{m}) \odot \mathbf{z}_{t-1}^{bg}, \quad (4)$$

where \odot is element-wise multiplication and \mathbf{m} is downsampled to the latent resolution (details below).

Permissible Editing Strength via Two Timesteps. To explicitly allocate plasticity between regions, we use two timestep indices τ_{fg} and τ_{bg} (with $\tau_{fg} > \tau_{bg}$). Following an SDEdit-style initialization at $t = \tau_{fg}$, we enforce a plasticity gap during the interval $\tau_{fg} \geq t > \tau_{bg}$. In this phase, the foreground evolves freely via the diffusion model to accommodate non-rigid deformations, while the background is explicitly anchored to the source latent trajectory to suppress temporal flicker. Once $t \leq \tau_{bg}$, both regions are refined jointly to ensure boundary coherence.

5 Experiments

5.1 Experimental Settings

Baselines and Implementation Details. We evaluate five video editing models on NRVBench and Benchmark-V0, including Wan-Edit [Li *et al.*, 2025], TokenFlow [Geyer *et al.*, 2024], AnyV2V [Ku *et al.*, 2024], VidToMe [Li *et al.*, 2024] and Pyramid-Edit [Li *et al.*, 2025]. These methods represent two distinct paradigms: inversion-based pipelines (TokenFlow, AnyV2V, VidToMe) that perform DDIM inversion to obtain noisy latents, and inversion-free baselines (Wan-Edit, Pyramid-Edit) that directly leverage source priors. Wan-Edit is instantiated with the Wan2.1-T2V model. AnyV2V employs InstructPix2Pix [Brooks *et al.*, 2023] as its image editing backbone for the initial frame, and incorporates Plug-and-Play (PnP) features to guide structural consistency during propagation. Pyramid-Edit utilizes the 384P Pyramid-Flow backbone. All experiments are conducted on a single NVIDIA H20 GPU. Further baseline-specific details are deferred to the appendices *B*.

Methods	Structure		Background Preservation				Text Alignment		IQA	Motion	Speed
	Dist.($\times 10^3$) \downarrow	PSNR \uparrow	LPIPS($\times 10^3$) \downarrow	MSE($\times 10^4$) \downarrow	SSIM($\times 10^2$) \uparrow	CLIP-S \uparrow	CLIP-S _{edit} \uparrow	NIQE \downarrow	S.($\times 10^2$) \uparrow	FPS \uparrow	
Dataset V0 (15 \times 3 \times 150 frames)											
<i>Source Videos</i>	0	∞	0	0	100	28.11	25.83	8.23	80.14	/	
Wan-Edit \diamond [Li <i>et al.</i> , 2025]	18.04	32.36	96.76	7.99	95.66	27.52	24.41	10.70	60.06	2.03	
Pyramid-Edit \diamond [Li <i>et al.</i> , 2025]	84.06	22.41	128.14	77.72	87.78	27.68	24.99	9.58	57.95	1.47	
TokenFlow \dagger [Geyer <i>et al.</i> , 2024]	50.52	24.19	98.68	53.96	88.38	26.83	24.69	9.96	62.70	2.96	
VidToMe \dagger^* [Li <i>et al.</i> , 2024]	231.82	13.80	214.59	491.33	75.65	25.00	22.85	10.37	55.78	4.59	
AnyV2V \dagger [Ku <i>et al.</i> , 2024]	182.00	13.61	354.90	786.42	72.44	23.31	21.97	11.63	54.63	3.55	
VM-Edit (Ours)	16.45	37.35	58.91	2.99	97.36	27.87	25.48	9.04	43.69	2.34	
Dataset V1 (180 \times 60 frames)											
<i>Source Videos</i>	0	∞	0	0	100	26.66	23.83	7.37	90.83	/	
Wan-Edit \diamond [Li <i>et al.</i> , 2025]	17.66	29.37	111.92	17.35	92.15	26.63	23.24	8.28	60.65	2.67	
Pyramid-Edit \diamond [Li <i>et al.</i> , 2025]	83.30	21.73	147.40	95.24	84.50	26.65	22.47	8.26	53.89	2.78	
TokenFlow \dagger [Geyer <i>et al.</i> , 2024]	111.93	21.10	134.31	118.23	75.3	26.47	23.28	7.98	58.49	3.11	
VidToMe \dagger^* [Li <i>et al.</i> , 2024]	364.93	11.80	300.64	778.40	59.78	26.60	22.89	8.34	57.76	3.89	
AnyV2V \dagger [Ku <i>et al.</i> , 2024]	329.34	13.83	353.94	646.59	58.48	23.32	20.75	9.47	49.14	2.76	
VM-Edit (Ours)	8.69	35.79	47.89	4.74	95.72	26.15	23.19	7.36	60.94	2.21	

Table 2: Quantitative comparison on V0 and V1 benchmarks. **Source Videos** provide reference values. The best editing results are highlighted in **bold**. \diamond : Inversion-free methods, \dagger : Inversion-based methods, $*$: Token-Merging-based.

Method	$S_{phy} \uparrow$	$S_{temp} \uparrow$	$S_{instr} \uparrow$	NRVE-Acc \uparrow	Time (s) \downarrow
TokenFlow	71.00	45.78	67.50	33.05	0.32
Pyramid-Edit	65.00	44.56	75.28	32.20	0.36
Wan-Edit	73.22	54.56	60.65	36.88	0.37
VidToMe	70.56	46.00	68.61	33.80	0.26
AnyV2V	71.33	43.11	65.56	30.35	0.35
Ours	71.44	49.44	68.89	34.71	0.45

Table 3: Quantitative comparison on NRVBench using our proposed NRVE-Acc metrics. Underline indicates the second best.

Evaluation Metrics. We evaluate editing quality on NRVBench and its pilot benchmark through two complementary lenses: overall accuracy and fine-grained diagnostics. First, we report our proposed NRVE-Acc alongside inference efficiency (Table 3). Second, we employ a comprehensive diagnostic suite (Table 2) to isolate specific performance attributes: Structure Distance [Tumanyan *et al.*, 2022] for geometric deviation; Background Preservation metrics (PSNR \uparrow , LPIPS [Zhang *et al.*, 2018] \downarrow , MSE \downarrow , SSIM [Wang *et al.*, 2004] \uparrow) computed on the non-edited regions to measure context stability; Text Alignment (CLIP-Sim [Wu *et al.*, 2021] and CLIP-Sim_{edit}) to evaluate global and edit-specific prompt consistency; Image Quality Assessment (NIQE [Saad and Bovik, 2012] \downarrow) for no-reference visual quality; and Motion Fidelity Score [Yatim *et al.*, 2024] to characterize temporal coherence. For reference, we report metrics on the unedited *Source Videos*, which serve as an upper bound for structural and temporal fidelity.

5.2 Overall Results

Benchmark Results. Table 2 presents a quantitative comparison between VM-Edit and representative baselines on both V0 and V1 benchmarks. Several key observations emerge: (1) Superior Structure and Background Preservation: VM-Edit dominates in structural consistency. It achieves the lowest structure distance (8.69) and highest background metrics (35.79 PSNR / 95.72 SSIM), significantly outperforming all baselines on NRVBench. In contrast, propagation-based methods like AnyV2V suffer severe distortions, highlighting

the robustness of our region-wise strategy. (2) Competitive Text Alignment: Despite strict structural constraints, VM-Edit maintains competitive instruction alignment (CLIP-S 26.15), performing on par with the best baselines. (3) Robust Motion Fidelity: VM-Edit matches Wan-Edit in Motion Fidelity (60.94 vs. 60.65) and outperforms TokenFlow, VidToMe, and AnyV2V, proving its ability to handle complex non-rigid motion without sacrificing temporal consistency. A detailed category-wise breakdown is provided in Figure 4. (4) Practical Efficiency: VM-Edit balances quality with efficiency, achieving strong perceptual scores (NIQE 7.36) and a practical throughput of 2.21 FPS. Collectively, these results establish VM-Edit as the superior choice for non-rigid video editing, particularly in scenarios where preserving background integrity is a critical prerequisite.

Although not intended as a panacea for every non-rigid editing challenge, VM-Edit serves as a simple yet effective baseline for the non-rigid editing community. By stripping away complex propagation modules in favor of a straightforward dual-clock mechanism, it achieves superior background stability and structure preservation compared to elaborate training-free or propagation-based methods. While we acknowledge that its reliance on the source prior may limit the generation of extremely large-scale topological changes, VM-Edit successfully balances the trade-off between fidelity and plasticity, establishing a robust standard for future non-rigid video editing research.

Metrics and VM-Edit Results. NRVE-Acc Results. Table 3 reports our proposed NRVE-Acc and its three components (S_{phy} , S_{temp} , S_{instr}) together with per-frame inference time. On NRVBench, while Wan-Edit attains the highest overall score (36.88), our VM-Edit secures the second-best position (34.71), outperforming TokenFlow (33.05), Pyramid-Edit (32.20), VidToMe (33.80), and AnyV2V (30.35). While Wan-Edit achieves temporal consistency through full-frame generation, it fails to preserve background integrity. Quantitatively, this results in a 6.42 dB lower PSNR compared to our VM-Edit (see Table 2), highlighting the severity of the background drift. In contrast,

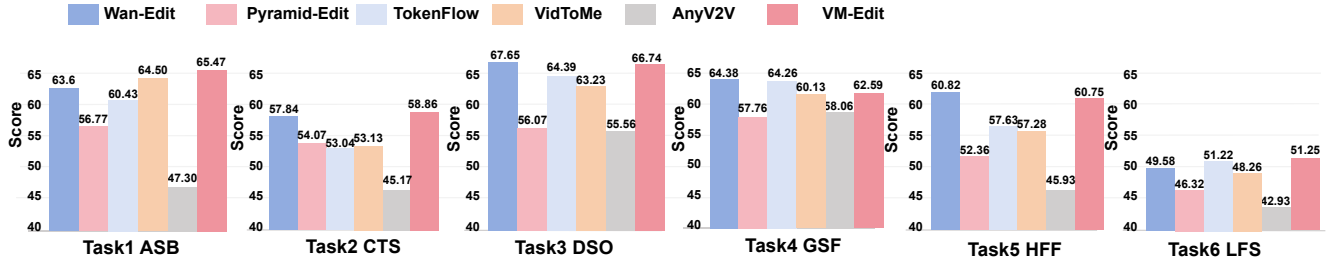


Figure 4: Comparison of six models across six non-rigid categories using Motion Fidelity (scaled by 10^2).

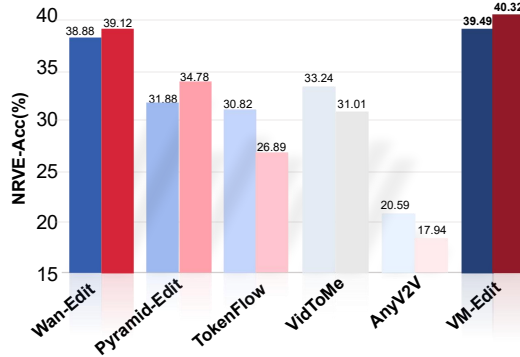


Figure 5: NRVE-Acc results (Left) and human evaluation (Right) on CTS. Detailed results are provided in the appendices D.

VM-Edit stands out as the sole approach capable of surgical non-rigid editing, executing precise local deformations while preserving pixel-level background stability. We argue that such fidelity is essential for practical editing scenarios, where maintaining the original context is often a stricter constraint than maximizing global fluidity. By leveraging mask guidance, VM-Edit secures the second-best performance across all three sub-tasks as well as the overall score. A current limitation is that VM-Edit involves selecting timestep indices for each video, a characteristic shared with prior region-controlled methods like TTM [Singer *et al.*, 2025]. To mitigate manual tuning efforts, we have empirically identified effective index ranges tailored to each non-rigid category and provide a systematic selection guide in appendices. Notably, the quantitative results reported in Table 2 were obtained using these fixed ranges for each of the six categories, avoiding per-video adjustments. This empirically demonstrates that VM-Edit achieves robust performance without the need for excessive per-video tuning. While this offers a robust practical heuristic, developing fully automatic and adaptive index scheduling remains an exciting and promising direction for future work.

5.3 Human Evaluation

Human validation of NRVE-Acc metrics. To verify the reliability of our metric, we conducted a stratified random sampling of ten source videos from each non-rigid target category, accompanied by five corresponding editing prompts

and four MCQs for each video. Human evaluators were tasked with answering the identical set of questions used by the VLM, after which we computed the averaged scores for comparison. We performed a detailed analysis of the alignment between human and model judgments. As illustrated in Figure 5, which specifically showcases the comparison within the CTS category, the human scores exhibit a high degree of proximity to Qwen-2.5-VL’s results. This quantitative agreement shows that NRVE-Acc maintains excellent compatibility with human perception and provides a consistent standard for evaluation. Meanwhile, methods based on editing the first frame often yield lower human evaluation scores, which corroborates our hypothesis. The cross-category comparison reveals that the VLM exhibits more severe misjudgments in the HFF category.

Human validation of data. We adopt a human-in-the-loop pipeline where initial masks generated by SAM2 undergo rigorous manual refinement. This ensures pixel-perfect alignment with target regions, guaranteeing high-quality ground truth for reliable evaluation. To determine the optimal timestep indices (τ_{fg} and τ_{bg}) for VM-Edit, we conducted a grid search involving at least five distinct combinations for each video. The final parameters were selected via human visual inspection, strictly prioritizing the configuration that maximized foreground editing plasticity while maintaining minimal background alteration.

6 Conclusion

In this paper, we introduce a comprehensive framework to tackle the inherent challenges of physical plausibility and temporal consistency in non-rigid video editing. By introducing NRVBench, we offer a dedicated benchmark for non-rigid video editing with physics-grounded categories, fine-grained instructions, and masks to reveal current failures in physical realism and temporal consistency. To rigorously quantify progress, we introduce NRVE-Acc, a VLM-based metric that jointly evaluates instruction alignment, physical plausibility, and temporal consistency using structured QA and motion cues. Furthermore, our proposed VM-Edit validates the efficacy of region-conditioned sampling, demonstrating that a training-free, structure-aware mechanism can effectively tackle non-rigid motion, achieving superior performance in both general and physics-specific metrics.

References

[Avrahami *et al.*, 2022] Omri Avrahami, Dani Lischinski, and Ohad Fried. Blended diffusion for text-driven editing of natural images. In *Proceedings of the IEEE/CVF Conference on Computer Vision and Pattern Recognition*, pages 18187–18197, 2022.

[Blattmann *et al.*, 2023] Andreas Blattmann, Tim Dockhorn, Sumith Kulal, Daniel Mendelevitch, Maciej Kilian, Dominik Lorenz, Yam Levi, Zion English, Vikram Voleti, Adam Letts, et al. Stable video diffusion: Scaling latent video diffusion models to large datasets. *arXiv preprint arXiv:2311.15127*, 2023.

[Brooks *et al.*, 2023] Tim Brooks, Aleksander Holynski, and Alexei A. Efros. Instructpix2pix: Learning to follow image editing instructions. In *Proceedings of the IEEE/CVF Conference on Computer Vision and Pattern Recognition*, pages 18392–18402, 2023.

[Chang *et al.*, 2025] Di Chang, Mingdeng Cao, Yichun Shi, Bo Liu, Shengqu Cai, Shijie Zhou, Weilin Huang, Gordon Wetzstein, Mohammad Soleymani, and Peng Wang. Bytemorph: Benchmarking instruction-guided image editing with non-rigid motions. *arXiv preprint arXiv:2506.03107*, 2025.

[Deng *et al.*, 2024] Yufan Deng, Ruida Wang, Yuhao Zhang, Yu-Wing Tai, and Chi-Keung Tang. Dragvideo: Interactive drag-style video editing. pages 183–199, 2024.

[Feng *et al.*, 2024] Ruoyu Feng, Wenming Weng, Yanhui Wang, Yuhui Yuan, Jianmin Bao, Chong Luo, Zhibo Chen, and Baining Guo. Ccredit: Creative and controllable video editing via diffusion models. In *Proceedings of the IEEE/CVF Conference on Computer Vision and Pattern Recognition*, pages 6712–6722, 2024.

[Feng *et al.*, 2025] Kunyu Feng, Yue Ma, Bingyuan Wang, Chenyang Qi, Haozhe Chen, Qifeng Chen, and Zeyu Wang. Dit4edit: Diffusion transformer for image editing. In *Proceedings of the AAAI Conference on Artificial Intelligence*, volume 39, pages 2969–2977, 2025.

[Geyer *et al.*, 2024] Michal Geyer, Omer Bar-Tal, Shai Bagon, and Tali Dekel. Tokenflow: Consistent diffusion features for consistent video editing. In *International Conference on Learning Representations*, 2024.

[Koo *et al.*, 2024] Gwanhyeong Koo, Sunjae Yoon, Ji Woo Hong, and Chang D Yoo. Flexedit: Frequency-aware latent refinement for enhanced non-rigid editing. In *European Conference on Computer Vision*, pages 363–379. Springer, 2024.

[Ku *et al.*, 2024] Max Ku, Cong Wei, Weiming Ren, Huan Yang, and Wenhui Chen. Anyv2v: A tuning-free framework for any video-to-video editing tasks. *Transactions on Machine Learning Research*, 2024.

[Li *et al.*, 2024] Xirui Li, Chao Ma, Xiaokang Yang, and Ming-Hsuan Yang. Vidtome: Video token merging for zero-shot video editing. In *Proceedings of the IEEE/CVF Conference on Computer Vision and Pattern Recognition*, pages 7486–7495, 2024.

[Li *et al.*, 2025] Minghan Li, Chenxi Xie, Yichen Wu, Lei Zhang, and Mengyu Wang. Five-bench: A fine-grained video editing benchmark for evaluating emerging diffusion and rectified flow models. In *Proceedings of the IEEE/CVF International Conference on Computer Vision*, pages 16672–16681, 2025.

[Lugmayr *et al.*, 2022] Andreas Lugmayr, Martin Danelljan, Andres Romero, Fisher Yu, Radu Timofte, and Luc Van Gool. Repaint: Inpainting using denoising diffusion probabilistic models. In *Proceedings of the IEEE/CVF Conference on Computer Vision and Pattern Recognition*, pages 11461–11471, June 2022.

[Ma *et al.*, 2025] Guoqing Ma, Haoyang Huang, Kun Yan, Liangyu Chen, Nan Duan, Shengming Yin, Changyi Wan, Ranchen Ming, Xiaoniu Song, Xing Chen, et al. Step-video-t2v technical report: The practice, challenges, and future of video foundation model. *arXiv preprint arXiv:2502.10248*, 2025.

[Mou *et al.*, 2024] Chong Mou, Mingdeng Cao, Xintao Wang, Zhaoyang Zhang, Ying Shan, and Jian Zhang. Revideo: Remake a video with motion and content control. volume 37, pages 18481–18505, 2024.

[OpenAI *et al.*, 2024] OpenAI, Aaron Hurst, Adam Lerer, Adam P. Goucher, Adam Perelman, Aditya Ramesh, Aidan Clark, A. J. Ostrow, Akila Welihinda, Alan Hayes, Alec Radford, et al. Gpt-4o system card. *arXiv preprint arXiv:2410.21276*, 2024.

[Ouyang *et al.*, 2024] Hao Ouyang, Qiuyu Wang, Yuxi Xiao, Qingyan Bai, Juntao Zhang, Kecheng Zheng, Xiaowei Zhou, Qifeng Chen, and Yujun Shen. CoDef: Content deformation fields for temporally consistent video processing. In *Proceedings of the IEEE/CVF Conference on Computer Vision and Pattern Recognition*, pages 8089–8099, 2024.

[Perazzi *et al.*, 2016] Federico Perazzi, Jordi Pont-Tuset, Brian McWilliams, Luc Van Gool, Markus Gross, and Alexander Sorkine-Hornung. A benchmark dataset and evaluation methodology for video object segmentation. In *Proceedings of the IEEE Conference on Computer Vision and Pattern Recognition*, pages 724–732, 2016.

[Qi *et al.*, 2023] Chenyang Qi, Xiaodong Cun, Yong Zhang, Chenyang Lei, Xintao Wang, Ying Shan, and Qifeng Chen. Fatezero: Fusing attentions for zero-shot text-based video editing. In *Proceedings of the IEEE/CVF International Conference on Computer Vision*, pages 15932–15942, 2023.

[Ravi *et al.*, 2024] Nikhila Ravi, Valentin Gabeur, Yuan-Ting Hu, Ronghang Hu, Chaitanya Ryali, Tengyu Ma, Haitham Khedr, Roman Rädle, Chloe Rolland, Laura Gustafson, et al. Sam 2: Segment anything in images and videos. *arXiv preprint arXiv:2408.00714*, 2024.

[Rombach *et al.*, 2022] Robin Rombach, Andreas Blattmann, Dominik Lorenz, Patrick Esser, and Björn Ommer. High-resolution image synthesis with latent diffusion models. In *Proceedings of the IEEE/CVF*

Conference on Computer Vision and Pattern Recognition, pages 10684–10695, 2022.

[Saad and Bovik, 2012] Michele A. Saad and Alan C. Bovik. Blind quality assessment of videos using a model of natural scene statistics and motion coherency. In *2012 Conference Record of the Forty Sixth Asilomar Conference on Signals, Systems and Computers (ASILOMAR)*, pages 332–336, 2012.

[Singer *et al.*, 2024] Uriel Singer, Amit Zohar, Yuval Kirstain, Shelly Sheynin, Adam Polyak, Devi Parikh, and Yaniv Taigman. Video editing via factorized diffusion distillation. In *European Conference on Computer Vision*, pages 450–466. Springer, 2024.

[Singer *et al.*, 2025] Assaf Singer, Noam Rotstein, Amir Mann, Ron Kimmel, and Or Litany. Time-to-move: Training-free motion controlled video generation via dual-clock denoising. *arXiv preprint arXiv:2511.08633*, 2025.

[Sun *et al.*, 2024] Wenhao Sun, Rong-Cheng Tu, Jingyi Liao, and Dacheng Tao. Diffusion model-based video editing: A survey. *arXiv preprint arXiv:2407.07111*, 2024.

[Team Wan *et al.*, 2025] Team Wan, Ang Wang, Baole Ai, Bin Wen, Chaojie Mao, Chen-Wei Xie, Di Chen, Feiwu Yu, Haiming Zhao, Jianxiao Yang, et al. Wan: Open and advanced large-scale video generative models. *arXiv preprint arXiv:2503.20314*, 2025.

[Tu *et al.*, 2024] Shuyuan Tu, Qi Dai, Zhi-Qi Cheng, Han Hu, Xintong Han, Zuxuan Wu, and Yu-Gang Jiang. Motioneeritor: Editing video motion via content-aware diffusion. In *Proceedings of the IEEE/CVF Conference on Computer Vision and Pattern Recognition*, pages 7882–7891, 2024.

[Tu *et al.*, 2025] Shuyuan Tu, Qi Dai, Zihao Zhang, Sicheng Xie, Zhi-Qi Cheng, Chong Luo, Xintong Han, Zuxuan Wu, and Yu-Gang Jiang. Motionfollower: Editing video motion via score-guided diffusion. In *Proceedings of the IEEE/CVF International Conference on Computer Vision*, pages 12822–12831, October 2025.

[Tumanyan *et al.*, 2022] Narek Tumanyan, Omer Bar-Tal, Shai Bagon, and Tali Dekel. Splicing vit features for semantic appearance transfer. In *Proceedings of the IEEE/CVF Conference on Computer Vision and Pattern Recognition*, pages 10748–10757, 2022.

[Wang *et al.*, 2004] Zhou Wang, Alan C. Bovik, Hamid R. Sheikh, and Eero P. Simoncelli. Image quality assessment: from error visibility to structural similarity. *IEEE Transactions on Image Processing*, 13(4):600–612, 2004.

[Wang *et al.*, 2024] Wen Wang, Yan Jiang, Kangyang Xie, Zide Liu, Hao Chen, Yue Cao, Xinlong Wang, and Chunhua Shen. Zero-shot video editing using off-the-shelf image diffusion models. *arXiv preprint arXiv:2303.17599*, 2024.

[Wu *et al.*, 2021] Chenfei Wu, Lun Huang, Qianxi Zhang, Binyang Li, Lei Ji, Fan Yang, Guillermo Sapiro, and Nan Duan. Godiva: Generating open-domain videos from natural descriptions. *arXiv preprint arXiv:2104.14806*, 2021.

[Wu *et al.*, 2023a] Jay Zhangjie Wu, Yixiao Ge, Xintao Wang, Stan Weixian Lei, Yuchao Gu, Yufei Shi, Wynne Hsu, Ying Shan, Xiaohu Qie, and Mike Zheng Shou. Tune-a-video: One-shot tuning of image diffusion models for text-to-video generation. In *Proceedings of the IEEE/CVF international conference on computer vision*, pages 7623–7633, 2023.

[Wu *et al.*, 2023b] Jay Zhangjie Wu, Xiuyu Li, Difei Gao, Zhen Dong, Jinbin Bai, Aishani Singh, Xiaoyu Xiang, Youzeng Li, Zuwei Huang, Yuanxi Sun, et al. CVPR 2023 text guided video editing competition. *arXiv preprint arXiv:2310.16003*, 2023.

[Wu *et al.*, 2025] Jay Zhangjie Wu, Guian Fang, Dongrong Joe Fu, Vijay Anand Raghava Kanakagiri, Forrest Iandola, Kurt Keutzer, Wynne Hsu, Zhen Dong, and Mike Zheng Shou. Veditbench: Holistic benchmark for text-guided video editing, 2025.

[Yang *et al.*, 2023] Shuai Yang, Yifan Zhou, Ziwei Liu, and Chen Change Loy. Rerender a video: Zero-shot text-guided video-to-video translation. In *SIGGRAPH Asia 2023 Conference Papers*, 2023.

[Yang *et al.*, 2025] Xiangpeng Yang, Linchao Zhu, Hehe Fan, and Yi Yang. Videograin: Modulating space-time attention for multi-grained video editing. In *International Conference on Learning Representations*, 2025.

[Yatim *et al.*, 2024] Danah Yatim, Rafail Fridman, Omer Bar-Tal, Yoni Kasten, and Tali Dekel. Space-time diffusion features for zero-shot text-driven motion transfer. In *Proceedings of the IEEE/CVF Conference on Computer Vision and Pattern Recognition*, pages 8466–8476, 2024.

[Yoon *et al.*, 2024] Sunjae Yoon, Gwanhyeong Koo, Ji Woo Hong, and Chang D Yoo. Dni: Dilutional noise initialization for diffusion video editing. In *European Conference on Computer Vision*, pages 180–195. Springer, 2024.

[Zhang *et al.*, 2018] Richard Zhang, Phillip Isola, Alexei A. Efros, Eli Shechtman, and Oliver Wang. The unreasonable effectiveness of deep features as a perceptual metric. In *Proceedings of the IEEE Conference on Computer Vision and Pattern Recognition*, pages 586–595, 2018.

[Zhong *et al.*, 2024] Xiaojing Zhong, Xinyi Huang, Xiaofeng Yang, Guosheng Lin, and Qingyao Wu. Deco: Decoupled human-centered diffusion video editing with motion consistency. In *European Conference on Computer Vision*, pages 352–370. Springer, 2024.

[Zhu *et al.*, 2025] Yixuan Zhu, Haolin Wang, Shilin Ma, Wenliang Zhao, Yansong Tang, Lei Chen, and Jie Zhou. FADE: Frequency-aware diffusion model factorization for video editing. In *Proceedings of the IEEE/CVF Conference on Computer Vision and Pattern Recognition*, pages 28426–28435, 2025.

A NRVBench framework

A.1 More Details on NRVBench Dataset

The construction of the NRVBench involves the collection of real-world videos, the generation templates of the prompts, the filtering rules and manual verification processes, as shown in Figure 6 and Figure 7.

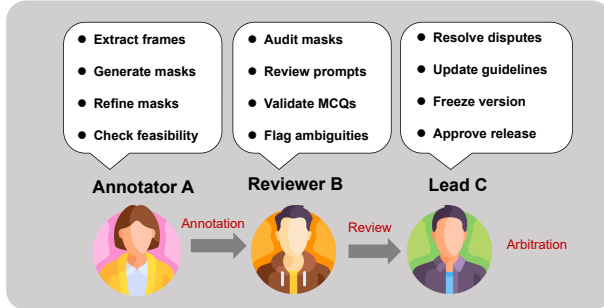


Figure 6: Manual Verification Processes.

Collection of videos. We begin by selecting real-world videos from the DAVIS [Perazzi *et al.*, 2016] dataset and Pexels that are well-suited for non-rigid video editing. For each chosen video, we use GPT-4o [OpenAI *et al.*, 2024] to generate detailed annotations every 15 frame, capturing key elements such as non-rigid dynamics, object categories, and camera movements. Next, we create fine-grained editing instructions and source/target prompts, which are paired with dense segmentation masks derived from SAM2 [Ravi *et al.*, 2024] to support structure-aware evaluation. The full construction process and examples of the benchmark entries are shown in Figure 7. In this process, human justification is involved in assessing the quality of both the segmentation masks and the physical plausibility of instructions to ensure the generation of a high-quality, physics-grounded benchmark.

Prompt Generation Templates. For the verified video-caption pairs, we design specialized meta-prompts to synthesize target editing instructions across six non-rigid physical categories (e.g., Fluidity, Elasticity). GPT-4o is employed to transmute the original descriptive captions into dynamic target prompts by injecting category-specific deformation constraints while preserving the background context. Figure 8 and table 1 illustrates the prompt framework and provides concrete examples of the mapping from source captions to physics-grounded editing instructions.

Filtering Rules. To ensure high visual fidelity, consistent temporal structure, and unambiguous evaluation targets, we apply a set of strict filtering rules to all candidate videos before annotation. First, we retain only videos with a spatial resolution of at least 720p, which provides sufficient detail for pixel-accurate masks and reduces evaluation noise for fine non-rigid structures. We discard samples containing prominent watermarks, large subtitles, or stickers that occlude the target object for a non-trivial portion of frames, as such overlays confound both editing and

downstream assessment. We further remove videos with severe compression artifacts (e.g., strong blocking, ringing, or excessive quantization noise) that degrade boundary visibility or introduce spurious temporal inconsistencies. Second, we prefer single-shot segments to avoid abrupt viewpoint changes; clips with evident shot transitions are excluded or re-trimmed to a continuous single-shot interval. Finally, we enforce a single-primary-target constraint: each clip must contain one clearly identifiable main editing subject that remains trackable throughout the selected segment. We allow composite-material scenes (e.g., a person wearing clothes), but require annotators to assign exactly one primary evaluation category per clip (corresponding to the dominant non-rigid attribute under evaluation), while other materials are treated as contextual or secondary factors to prevent category ambiguity.

Manual Verification Processes. We adopt a three-role manual verification workflow to guarantee pixel-level mask quality, category consistency, and unambiguous instruction/QA design. **Annotator A** performs primary annotation, including mask refinement, category confirmation, and instruction feasibility checking. Given an input video, we first use ffmpeg to extract and trim a standardized frame sequence, after which SAM2 is used to generate an initial per-frame mask that serves as the annotation starting point. Annotator A then refines masks to ensure accurate boundaries and temporally consistent object identity, and verifies that the associated editing instruction is feasible and visually verifiable for the specified target and its physical/material properties. **Reviewer B** conducts an independent pass to audit the consistency and potential ambiguity of mask/prompt/MCQs triplets, focusing on common failure modes such as boundary jitter, background leakage into the target mask, unclear target references, non-observable changes, and MCQs with non-mutually exclusive options or multiple plausible answers. When disagreements arise, **Lead** serves as an adjudicator: resolving conflicts, updating annotation guidelines to reduce future variance, and freezing the finalized version of the sample once it meets quality criteria, as shown in Figure 6. For challenging categories, we adopt category-specific rules to improve reproducibility. For **HFF** (hair/feather-like structures), we annotate only the main hair/feather mass rather than individual strands, and explicitly follow a boundary policy centered on the dominant visible region. For **LFS/GSF** (gas-like phenomena), we prioritize the visible core body (e.g., the main liquid surface or dense smoke plume) and avoid including transparent or semi-transparent trailing wisps, which are inherently ambiguous and would reduce cross-annotator consistency and evaluation repeatability.

A.2 Six Non-Rigid Target Categories

To cover diverse non-rigid editing regimes, we taxonomize our benchmark into six categories based on physical properties, assigning specific physics criteria to each:

- **ASB** (Articulated Soft Bodies): Emphasizes joint constraints to penalize unrealistic limb distortion.

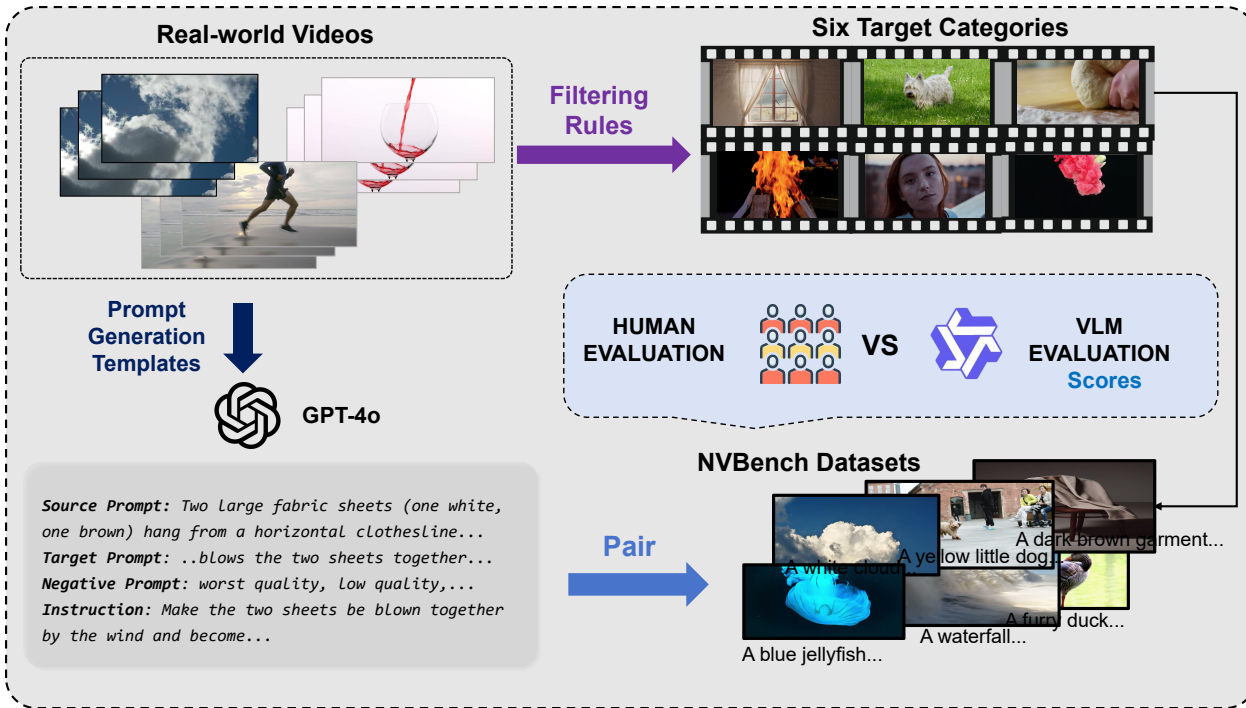


Figure 7: NRVBench Framework.

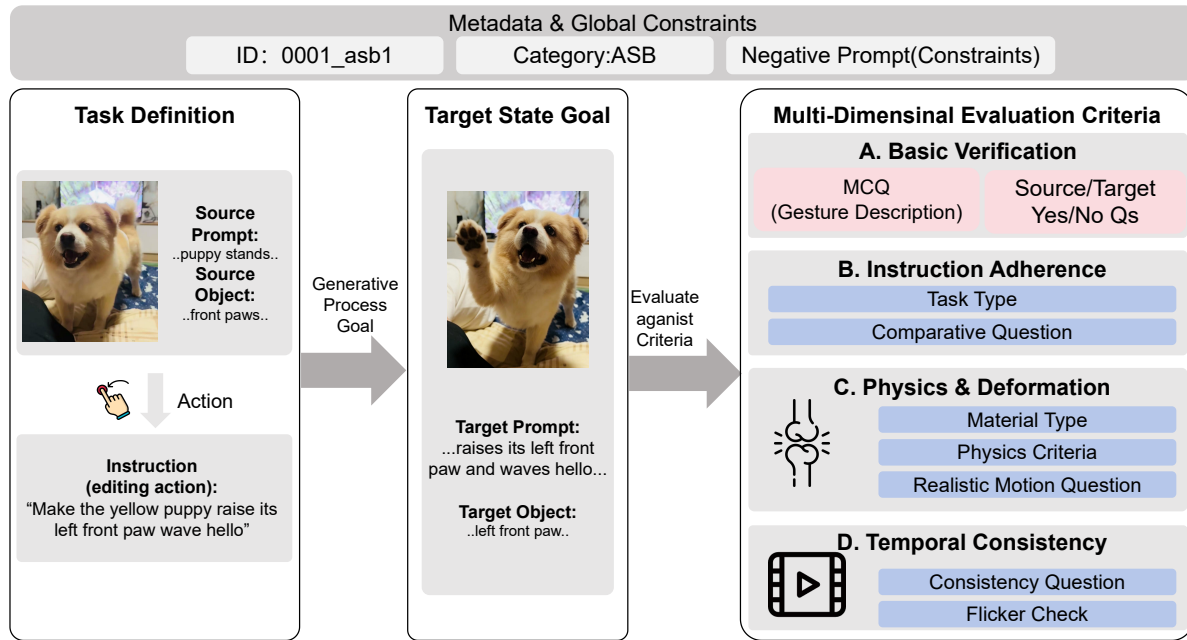


Figure 8: Dataset Construction Processes.

Method	Publication	Base T2I/V Model
TokenFlow [Geyer <i>et al.</i> , 2024]	ICCV23	SD2.1
AnyV2V [Ku <i>et al.</i> , 2024]	TMLR24	I2VGen-XL
VidToMe [Li <i>et al.</i> , 2024]	CVPR2024	SD1.5
Pyramid-Edit [Li <i>et al.</i> , 2025]	ICCV2025	Pyramid-Flow
Wan-Edit [Li <i>et al.</i> , 2025]	ICCV2025	Wan2.1
VM-Edit	-	Wan2.2

Table 4: Methods, publication venues, and base T2I/V models.

- **CTS** (Cloth and Thin-Shells): Focuses on surface continuity to penalize tearing artifacts and texture jitter.
- **HFF** (Hair/Fur/Feathers): Prioritizes strand coherence to detect density flickering in fine, fibrous structures.
- **LFS** (Liquids Free Surfaces): Enforces volume conservation and fluidity to avoid frozen-flow artifacts.
- **GSF** (Gas/Smoke/Fire): Highlights turbulence coherence, favoring natural topological evolution over rigid translational motion.
- **DSO** (Deformable Solid Objects): Validates elastic recovery and shape integrity under deformation.

B Baselines Comparison

B.1 Baselines

The method information under default settings in Table 4

Wan-Edit. Wan-Edit [Li *et al.*, 2025] is a training-free and inversion-free text-guided video editing baseline built upon recent Rectified Flow (RF) text-to-video generators. It adapts the inversion-free FlowEdit formulation to an RF-based T2V backbone (Wan2.1) and leverages the strong temporal prior of full-frame video generation to maintain smooth motion and coherent appearance over time. Since Wan2.1 follows a DiT-style design that processes multi-frame latents with self-attention, the FlowEdit-style editing mechanism can be integrated without introducing extra propagation modules or additional conditions (e.g., depth or segmentation), resulting in a lightweight inference pipeline. In practice, Wan-Edit is often competitive in temporal smoothness, while its full-frame generation nature may introduce background drift under strict structure-preservation requirements.

Pyramid-Edit. Pyramid-Edit [Li *et al.*, 2025] is an RF-based, training-free and inversion-free video editing baseline adapted from Pyramid-Flow. Unlike DiT-based backbones, Pyramid-Flow adopts a multi-resolution and temporally autoregressive pyramid architecture; therefore, the FlowEdit mechanism must be modified to support multi-resolution processing and to remain compatible with pyramid-level latent evolution. Pyramid-Edit further exploits temporal dependencies by conditioning later frames on historical (previous-frame) source or edited information within the noise-estimation network, which helps stabilize temporal consistency across long sequences. Similar to other RF-based approaches, Pyramid-Edit avoids expensive inversion and extra guidance inputs, providing an efficient baseline for prompt-driven edits.

TokenFlow. TokenFlow [Geyer *et al.*, 2024] is a training-free framework that repurposes a pre-trained text-to-image diffusion model for text-driven video editing. The key insight is that temporal consistency in RGB correlates with consistency in the diffusion feature space; TokenFlow enforces consistency by explicitly propagating diffusion features using inter-frame correspondences that are available in the model’s internal representations. Concretely, it (i) performs DDIM inversion per frame and extracts self-attention tokens across timesteps, (ii) computes inter-frame correspondences via nearest-neighbor matching in feature/token space, and (iii) alternates during denoising between random keyframe joint editing and token propagation from keyframes to all frames. A known limitation is that, because propagation is tied to the original feature correspondences, TokenFlow is less suitable for edits requiring substantial structural changes.

VidToMe. VidToMe [Li *et al.*, 2024] is a training-free, zero-shot video editing method that repurposes a pre-trained text-to-image diffusion model and improves temporal consistency by merging self-attention tokens across frames while reducing the quadratic memory cost of multi-frame attention. Concretely, it (i) performs DDIM inversion on each source frame to obtain the initial noisy latents, and can be combined with off-the-shelf image editing controllers (e.g., PnP/ControlNet/depth-conditioned diffusion) to preserve source structure; (ii) at each denoising step, randomly splits frames into chunks and applies intra-chunk local token merging for short-term continuity plus inter-chunk global token merging to prevent long-term content drift; and (iii) unmerges tokens after self-attention to restore per-frame tokens without modifying the self-attention operator itself. Token alignment is done by ToMe-style bipartite soft matching based on token similarity to merge temporally corresponding tokens. A practical limitation is that the method relies on reliable temporal correspondence for token matching, and overly aggressive merging (especially in deeper blocks) can degrade generation fidelity.

AnyV2V. AnyV2V [Ku *et al.*, 2024] is a tuning-free unified framework that decomposes video-to-video editing into two stages: (1) edit the first frame using any off-the-shelf (possibly black-box) image editing method or manual editing, and (2) animate the edited first frame with an image-to-video (I2V) generation model while preserving the source video’s motion and structure. To align the generated video with the source, AnyV2V employs DDIM inversion on the source video to obtain inverted latents as structural guidance, and injects intermediate features into the I2V model (spatial feature injection for background/structure, plus temporal feature injection for motion). This design makes AnyV2V broadly compatible with diverse edit types without parameter tuning, though its quality is naturally bounded by the chosen first-frame editor and the underlying I2V backbone.

B.2 Baselines Implementation Details.

All experiments were conducted using the official GitHub repository and environment, with default settings.

We evaluate AnyV2V under the prompt-based editing setting using an image-to-video backbone (i2vgen-xl). The

Algorithm 1 Data Generation & Evaluation Pipeline for Deformable Solid Objects (DSO)

Require: Source Video V_{src} , Source Caption C_{src}
Ensure: Target Edit Entry E_{edit}
Define Editing Guidelines (DSO Category):
Content Structure: Object + Non-Rigid Action + Environment + Camera Movement

Object Constraints:

- Maintain core identity but emphasize flexible material properties (e.g., fabric, rubber, hair).
- Object must remain solid but capable of shape change.

Action Constraints:

- Use physics-based deformations (bending, twisting, swaying, crumpling).
- **Avoid:** Fluid dynamics (melting) or rigid motion (sliding).

Camera & Env: Maintain original trajectory; keep background strictly unchanged.

Input Processing:

$$V_{src_id} \leftarrow "0074_dso14"$$

 $C_{src} \leftarrow "A \text{ hand holds up a bunch of flat pasta noodles which dangle down loosely...}"$
Target Prompt Generation:
Instruction: "Turn the pasta noodles in the hand into strands of hair"

$$C_{tgt} \leftarrow \text{ApplyEdit}(C_{src}, "pasta \text{ noodles}" \rightarrow "strands \text{ of hair}")$$

Result: "A hand holds up a bunch of long, dark strands of hair which dangle down loosely..."

Construct Evaluation Metrics (QA):
Identity Check (VQA):
 $Q_{src}: \text{"Is the hand holding pasta noodles?"} \rightarrow \text{Yes}$
 $Q_{tgt}: \text{"Is the hand holding strands of hair?"} \rightarrow \text{Yes}$
 $Q_{MC}: \text{"What is the hand holding?" Options: [a) Flat pasta noodles, b) Strands of hair]}$
Deformation Physics Check:
 $Criteria \leftarrow [\text{"strand_separation"}, \text{"texture_fidelity"}, \text{"gravity_compliance"}]$
 $Q_{phy}: \text{"Does the material look like fine, organic hair strands... without merging into a solid block?"}$
Temporal Consistency Check:
 $Q_{temp}: \text{"Across frames, does the hair texture remain consistent... or flicker back to pasta?"}$
 $Q_{flicker}: \text{"Are individual strands temporally coherent without excessive jitter?"}$
Output Generation:

$$E_{edit} \leftarrow \text{Compile}(V_{src_id}, C_{src}, C_{tgt}, Guidelines, QA_Metrics)$$

Return E_{edit}

video clip length is set to frames is 32 with a target frame rate of 8 FPS. We run TokenFlow with a fixed random seed on one GPU. Each evaluation clip contains 40 frames. Following the standard TokenFlow pipeline, we first obtain inversion latents using a DDIM-based inversion procedure with 500 inversion steps. For text-guided editing, we use Stable Diffusion v2.1 as the underlying diffusion backbone. The backbone model is Pyramid-Flow with a fixed input resolution of 384p. For each clip, the maximum number of processed frames is set to 41. The rectified-flow editing process uses 20 sampling timesteps. For VideToMe model, we use Stable Diffusion v1.5 and set inversion steps to 50 and a control scale to 1, which we apply pnp control in generation.

C VM-Edit

C.1 Permissible Editing Strength via Two Timesteps.

Following the dual-clock principle of TTM, we introduce two timestep indices τ_{fg} and τ_{bg} (with $\tau_{fg} > \tau_{bg}$) to explicitly allocate plasticity between regions *without* changing the global diffusion schedule. Intuitively, τ_{fg} controls how early the foreground is allowed to deviate, while τ_{bg} determines

how long the background remains anchored to the source prior.

Specifically, we adopt an SDEdit-style initialization strategy to preserve the source layout. We initialize sampling at step $t = \tau_{fg}$ by injecting noise into the source latent: $\mathbf{z}_{\tau_{fg}} := \mathbf{z}_{\tau_{fg}}^{src}$, and then execute the reverse diffusion process from $t = \tau_{fg}$ down to $t = 0$. During this generation phase, we define region-specific updates:

$$\mathbf{z}_{t-1}^{fg} = \hat{\mathbf{z}}_{t-1} \quad (\text{foreground edit}) \quad (5)$$

$$\mathbf{z}_{t-1} \leftarrow \mathbf{m} \odot \mathbf{z}_{t-1}^{fg} + (\mathbf{1} - \mathbf{m}) \odot \mathbf{z}_{t-1}^{bg}, \quad (6)$$

$$\mathbf{z}_{t-1}^{bg} = \begin{cases} \mathbf{z}_{t-1}^{src} & \text{if } t > \tau_{bg} \quad (\text{background anchor}) \\ \hat{\mathbf{z}}_{t-1} & \text{if } t \leq \tau_{bg} \quad (\text{background refinement}) \end{cases} \quad (7)$$

Combined with Eq. (4), this creates a plasticity gap in the interval $\tau_{fg} \geq t > \tau_{bg}$. In this phase, the foreground evolves freely via the model update while the background is *explicitly anchored* to \mathbf{z}^{src} , suppressing background jitter and temporal flicker. Once $t \leq \tau_{bg}$, both regions are refined jointly to improve boundary coherence. Larger τ_{fg} increases

foreground freedom for large-magnitude deformations, while smaller τ_{bg} enforces stronger background stability. We fix τ_{fg} and τ_{bg} for each video.

C.2 Systematic Guide for Timestep Index Selection

To facilitate the application of **VM-Edit** across diverse non-rigid scenarios, we provide a systematic guide for selecting the timestep indices τ_{fg} (controlling foreground editing plasticity) and τ_{bg} (controlling background preservation).

All indices are reported on a normalized scale of $0 \rightarrow 10$, where 0 represents the start of the diffusion process (noise) and 10 represents the end (clean image).

Design Philosophy: The Stability-Plasticity Trade-off

The selection of (τ_{fg}, τ_{bg}) is governed by the physical properties of the target deformation:

- **High τ (e.g., 8–10):** Required for amorphous substances (e.g., fire, water) where topological structures are constantly breaking and reforming.
- **Moderate τ (e.g., 5–8):** Suitable for flexible solids (e.g., cloth, rubber) that undergo large geometric warping but maintain surface continuity.
- **Low τ (e.g., 1–5):** Essential for articulated or fine-grained structures (e.g., bodies, hair) to prevent loss of identity or skeletal misalignment.

Category-Specific Reference Ranges

We have empirically identified optimal index ranges for the six primary categories defined in **NRVBench**.

ASB and HFF. These objects rely on strict skeletal structure (ASB) or dense, coherent texture patterns (HFF). Excessive editing steps often lead to broken limbs or flickering artifacts in fine details.

- Strategy: Tight Constrain. Keep τ_{fg} conservative to preserve the underlying biological or structural rig.
- Recommended Range: $\tau_{fg} \in [4, 6]$, $\tau_{bg} \in [2, 4]$.

CTS and DSO. These materials maintain continuous topology but undergo significant folding, bending, or stretching. They require enough freedom to change shape without turning into liquid.

- Strategy: Moderate Relaxation. A balanced range allows for crumpling (cloth) or squashing (dough) while maintaining object integrity.
- Recommended Range: $\tau_{fg} \in [6, 8]$, $\tau_{bg} \in [4, 6]$.

LFS and GSF. These categories involve chaotic, topology-breaking dynamics. The model must hallucinate entirely new shapes (e.g., splashes, billowing smoke) that do not exist in the source structure.

- Strategy: Maximum Plasticity. High τ_{fg} is essential to simulate phase transitions and turbulent flows.
- Recommended Range: $\tau_{fg} \in [8, 10]$, $\tau_{bg} \in [5, 7]$.

Summary Table

Table 5 summarizes the recommended default configurations based on our updated taxonomy.

Table 5: **Recommended Timestep Indices for NRVBench Categories.** Values are on a scale of 0–10. Categories are sorted by increasing requirement for plasticity.

Category (Abbr.)	Foreground (τ_{fg})		Background (τ_{bg})	
	Default	Range	Default	Range
<i>Group 1: High Structural Constraint</i>				
ASB (Articulated Soft Body)	5	4–6	3	2–4
HFF (Hair, Fur, Feathers)	5	4–6	3	2–4
<i>Group 2: Moderate Deformation</i>				
CTS (Cloth & Thin-Shell)	6	5–7	4	3–5
DSO (Deformable Solid)	7	6–8	5	4–6
<i>Group 3: High Plasticity / Fluidity</i>				
LFS (Liquid Free Surface)	9	8–10	6	5–7
GSF (Gas, Smoke, Fire)	9	8–10	6	5–7

Mask projection.

Spatial Layout mask sequence $\mathbf{M} \in \{0, 1\}^{T \times H \times W}$, where $\mathbf{M} = 1$ denotes the editable foreground (non-rigid target) and $\mathbf{M} = 0$ denotes the background context to be stabilized.

In our benchmark instantiation, \mathbf{M} is obtained from SAM2 [Ravi *et al.*, 2024]; We obtain a binary mask sequence \mathbf{M} in pixel space and project it to the latent resolution using nearest-neighbor interpolation; for backbones with temporal compression, we additionally subsample the mask sequence along time with nearest-neighbor to match the latent frame rate. To avoid human intervention, we compute per-frame candidate instance masks with SAM2 and select a single foreground track deterministically: we link instances across adjacent frames by maximum IoU matching, keep the longest/most persistent track, and set \mathbf{M}_t to the matched instance at each frame (ties broken by larger area). We optionally apply a light temporal smoothing to reduce boundary jitter. This produces a fully automated, reproducible \mathbf{M} for benchmarking. For a clean baseline, VM-Edit uses binary masks in Eq. (4). The same baseline can be straightforwardly generalized to soft masks or smoother blending schedules to further mitigate boundary artifacts (we leave this as an optional variant in ablations).

D NRVE-Acc

D.1 Temporal QA via Optical-Flow Visualization and VLM Scoring

Overview. Our video-level evaluation includes three QA-based components: (i) instruction-following QA, (ii) physics/deformation plausibility QA, and (iii) temporal coherence QA. All QA scores are produced by an open-source vision-language model (VLM) that returns either a discrete answer (for multiple-choice questions) or a Likert-style rating on a 1–5 scale (for plausibility and temporal stability). For temporal coherence, we additionally provide the VLM with an optical-flow visualization to make flicker and motion inconsistency more explicit than raw frames alone.

Frame triplet selection. Given a decoded video represented as a sequence of frames, we construct a temporal triplet by selecting the first frame, the middle frame, and the last frame. Concretely, for a video with T frames we

use indices $\{0, \lfloor T/2 \rfloor, T - 1\}$. This maximizes temporal spacing and highlights long-range temporal artifacts such as hallucination/teleportation and pronounced flicker.

Optical flow computation. We compute dense optical flow between consecutive frames in the triplet, i.e., between $(t \rightarrow t+k)$ and $(t+k \rightarrow t+2k)$. We adopt the classical Farnebäck method for dense optical flow with fixed hyper-parameters for reproducibility: pyramid scale 0.5, pyramid levels 3, window size 15, iterations 3, polynomial neighborhood size 5, polynomial smoothing 1.1, and no additional flags. All flows are computed on grayscale versions of the selected frames.

Flow visualization. For each flow field, we convert horizontal/vertical motion components into polar form (magnitude and direction) and visualize the result in an HSV encoding: hue represents motion direction and value represents motion magnitude. The magnitude is normalized to a fixed display range for visibility, while saturation is kept constant. We then convert the HSV representation to an RGB image. The two flow visualizations (for the first-to-middle and middle-to-last transitions) are concatenated horizontally into a single image, which serves as the input to the VLM for temporal coherence assessment.

Temporal coherence prompting and scoring. The temporal coherence prompt instructs the VLM to focus on frame-to-frame changes rather than single-frame quality, specifically checking for (i) temporal inconsistency such as disappearance, geometry jumps, or teleportation, and (ii) flicker or high-frequency texture/brightness jitter. The VLM outputs a single integer score in $\{1, 2, 3, 4, 5\}$, where 1 indicates severe temporal artifacts and 5 indicates perfectly coherent motion with no flicker. When the model is uncertain, it is encouraged to choose the lower (stricter) score to reduce false positives.

ROI handling for deformation plausibility. For deformation plausibility QA, we optionally restrict evaluation to a region of interest (ROI) derived from the provided segmentation masks. We compute per-frame bounding boxes with a small padding margin and take their union across the sampled frames to ensure a consistent crop region. Cropped frames share identical spatial extent before being fed to the VLM, which reduces background influence and focuses the judgment on the edited object.

Note on ROI for temporal QA. In the current setup, temporal coherence QA uses full-frame optical-flow visualization without ROI cropping, i.e., the flow is computed on the original frames and evaluated globally. If ROI-specific temporal evaluation is desired, one can first crop the sampled frames using the union ROI bounding box and then compute optical flow and its visualization on the cropped frames.

D.2 NRVE-Acc: Prompts, Templates, Sampling, and Parsing Rules

Judge prompts. We use Qwen2.5-VL-7B as an open-source judge and query it independently for three dimensions: instruction alignment, physical plausibility, and temporal consistency. Each query provides a compact visual input

(sampled frames or an auxiliary visualization) and a short task instruction. For instruction alignment, the judge answers a diagnostic multiple-choice question (MCQ). For physics and temporal evaluation, the judge outputs a single integer score from 1 to 5.

Evaluation templates. We employ two lightweight templates to constrain judge outputs. (1) For MCQ-based instruction evaluation, we ask the judge to select one option letter from the provided choices. (2) For Likert-style ratings, we instruct the judge to return only one digit in 1–5. These templates reduce verbosity and simplify deterministic parsing.

Sampling protocol. For instruction and physics evaluation, we uniformly sample a fixed number of frames from the decoded video frames. For temporal evaluation, we select a triplet of frames (first, middle, last) and compute two optical flows (first-to-middle and middle-to-last). We convert each flow to an HSV-based visualization, concatenate the two visualizations, and feed the resulting image to the judge to make flicker and motion discontinuities explicit. For physics evaluation, we optionally crop frames to the object region using the union bounding box derived from the provided masks.

MCQ construction. Each sample provides a diagnostic MCQ derived from the target instruction, designed to be directly verifiable from the edited video. The correct option is recorded as ground truth, and the judge’s selected option is compared against it to compute the instruction score.

Output-to-score parsing. For instruction alignment, we extract the first valid option letter from the judge output; the score is 1 if it matches the ground truth, 0.5 and 0 otherwise (option-to-score mapping can be extended when multi-level choices are used). For physics and temporal evaluation, we parse the first digit in 1–5 from the output; the rating is then linearly normalized to obtain a score in $[0, 1]$. Finally, we aggregate the three dimension scores using a geometric mean with uniform weights and a small numerical constant for stability, so a low score in any dimension reduces the overall NRVE-Acc.

D.3 Quantitative comparison table

We report the overall quantitative results on NRVBench V0/V1 using common video-editing metrics in Tab. 6, and summarize the overall NRVE-Acc scores (together with S_{phy} , S_{temp} , S_{instr} and per-frame inference time) in Tab. 7. For a finer-grained analysis on NRVBench V1, we provide per-category NRVE-Acc breakdowns for ASB, CTS, DSO, GSF, HFF, and LFS in Tables. 8–13, respectively. Moreover, low-level metric comparisons for each editing task (Edit 1–6) are presented in Tables. 14–19. To visually compare common metrics across methods, we plot Structure Distance, PSNR, LPIPS, MSE, SSIM, CLIP-S, and CLIP-S_{edit} in Figures. 9–15. Finally, we compare NRVE-Acc (left) with human evaluation (right) for ASB, CTS, DSO, GSF, HFF, and LFS in Figures. 16–21.

E Detailed Result Analysis for Table 2

Metric groups and interpretation. Table 2 reports metrics that jointly measure (i) structure preservation (Structure Dist., lower is better), (ii) background preservation on the unedited region (PSNR/SSIM higher; LPIPS/MSE lower), (iii) text alignment (CLIP-S on full frame and CLIP-S_{edit} on the edited region, higher), (iv) perceptual image quality (NIQE, lower), (v) motion fidelity (S., higher), and (vi) runtime (FPS, higher). Source Videos provide ideal reference values by comparing each source video with itself.

Dataset V0 (15 × 3 × 150 frames, brief). On the long-sequence V0 setting, VM-Edit yields the best structure fidelity (Structure Dist. 16.45), slightly outperforming Wan-Edit (18.04), and achieves the strongest background preservation across all four unedited-region metrics (PSNR 37.35, LPIPS 58.91, MSE 2.99, SSIM 97.36). It also attains the best text alignment (CLIP-S 27.87, CLIP-S_{edit} 25.48) and the best perceptual quality among edited methods (NIQE 9.04). The main trade-off is motion fidelity, where TokenFlow achieves the highest score (S. 62.70) while VM-Edit is lower (43.69), and runtime where inversion-based methods can be faster.

Dataset V1 analysis (180 × 60 frames). V1 is larger and more diverse, thus better reflecting robustness. Compared with V0, V1 also uses shorter clips (60 frames), reducing long-range accumulation but increasing diversity-induced difficulty. The results on V1 highlight several clear patterns:

(1) Stronger gains in structure and background preservation. VM-Edit achieves the best Structure Dist. (8.69), substantially outperforming the best baseline Wan-Edit (17.66) by 8.97 (about 50.8% relative reduction). For background preservation, VM-Edit again dominates all four metrics: PSNR 35.79 (+6.42 over Wan-Edit), LPIPS 47.89 (57.2% reduction vs Wan-Edit 111.92), MSE 4.74 (72.7% reduction vs Wan-Edit 17.35), and SSIM 95.72 (+3.57 over Wan-Edit). The coherent advantage across complementary metrics indicates that VM-Edit scales well to diverse videos while retaining precise edit localization.

(2) Text alignment is competitive but not always top-1. For CLIP-S (full frame), Pyramid-Edit is slightly higher (26.65) than VM-Edit (26.15), with a margin of 0.50. For CLIP-S_{edit}, TokenFlow is marginally higher (23.28) than VM-Edit (23.19), with a very small gap of 0.09. This suggests that some baselines can match or slightly exceed semantic alignment on either the full frame or the edited region, while VM-Edit remains highly competitive. Importantly, full-frame CLIP-S may under-represent localized edits when the changed region is small; CLIP-S_{edit} is more diagnostic for edit correctness, where VM-Edit remains near the top.

(3) Best perceptual quality (IQA). VM-Edit obtains the best NIQE (7.36) among edited methods and is essentially on par with the source reference (7.37). This indicates that VM-Edit introduces minimal perceptual degradation on average, improving over the next-best baseline TokenFlow by 0.62.

(4) Best motion fidelity on V1. Unlike V0, VM-Edit attains the highest motion score on V1 (S. 60.94), slightly surpassing Wan-Edit (60.65) by 0.29. Hence, under the V1 setting, VM-Edit preserves motion similarity while still

dominating structure/background metrics, demonstrating a stronger overall balance between spatial fidelity and temporal behavior than most baselines.

(5) Runtime remains a trade-off. TokenFlow is the fastest method (3.11 FPS), whereas VM-Edit runs at 2.21 FPS (slower by 0.90). VM-Edit is also slower than the inversion-free baselines Wan-Edit (2.67 FPS) and Pyramid-Edit (2.78 FPS). Therefore, the principal cost of VM-Edit is computation, while the gains in structure and background fidelity and perceptual quality are substantial and consistent.

Cross-dataset takeaway. Overall, VM-Edit provides the strongest spatial fidelity (structure and background) on both V0 and V1, achieves the best IQA and competitive text alignment, and reaches the best motion fidelity on V1. The results suggest VM-Edit is particularly suitable for benchmarking non-rigid edits that require strict preservation of non-edited regions, with runtime as the main trade-off.

Methods	Structure		Background Preservation				Text Alignment		IQA	Motion	Speed
	Dist. ($\times 10^3$) \downarrow	PSNR \uparrow	LPIPS ($\times 10^3$) \downarrow	MSE ($\times 10^4$) \downarrow	SSIM ($\times 10^2$) \uparrow	CLIP-S \uparrow	CLIP-S _{edit} \uparrow	NIQE \downarrow	S. ($\times 10^2$) \uparrow	FPS \uparrow	
Dataset V0 (15 \times 3 \times 150 frames)											
<i>Source Videos</i>	0	∞	0	0	100	28.11	25.83	8.23	80.14	/	
Wan-Edit \diamond [Li <i>et al.</i> , 2025]	18.04	32.36	96.76	7.99	95.66	27.52	24.41	10.70	60.06	2.03	
Pyramid-Edit \diamond [Li <i>et al.</i> , 2025]	84.06	22.41	128.14	77.72	87.78	27.68	24.99	9.58	57.95	1.47	
TokenFlow \dagger [Geyer <i>et al.</i> , 2024]	50.52	24.19	98.68	53.96	88.38	26.83	24.69	9.96	62.70	2.96	
VidToMe \dagger [Li <i>et al.</i> , 2024]	231.82	13.80	214.59	491.33	75.65	25.00	22.85	10.37	55.78	4.59	
AnyV2V \dagger [Ku <i>et al.</i> , 2024]	182.00	13.61	354.90	786.42	72.44	23.31	21.97	11.63	54.63	3.55	
VM-Edit (Ours)	16.45	37.35	58.91	2.99	97.36	27.87	25.48	9.04	43.69	2.34	
Dataset V1 (180 \times 60 frames)											
<i>Source Videos</i>	0	∞	0	0	100	26.66	23.83	7.37	90.83	/	
Wan-Edit \diamond [Li <i>et al.</i> , 2025]	17.66	29.37	111.92	17.35	92.15	26.63	23.24	8.28	60.65	2.67	
Pyramid-Edit \diamond [Li <i>et al.</i> , 2025]	83.30	21.73	147.40	95.24	84.50	26.65	22.47	8.26	53.89	2.78	
TokenFlow \dagger [Geyer <i>et al.</i> , 2024]	111.93	21.10	134.31	118.23	75.3	26.47	23.28	7.98	58.49	3.11	
VidToMe \dagger [Li <i>et al.</i> , 2024]	364.53	11.80	300.64	778.40	59.78	26.60	22.89	8.34	57.76	3.89	
AnyV2V \dagger [Ku <i>et al.</i> , 2024]	329.34	13.83	353.94	646.59	58.48	23.32	20.75	9.47	49.14	2.76	
VM-Edit (Ours)	8.69	35.79	47.89	4.74	95.72	26.15	23.19	7.36	60.94	2.21	

Table 6: Quantitative comparison on V0 and V1 benchmarks. **Source Videos** provide reference (ideal) values by comparing each source video with itself. The best editing results are highlighted in **bold**. \diamond : Inversion-free methods, \dagger : Inversion-based methods

Method	$S_{phy} \uparrow$	$S_{temp} \uparrow$	$S_{instr} \uparrow$	NRVE-Acc \uparrow	Time (s) \downarrow
Dataset V0					
Wan-Edit	67.89	55.11	72.22	33.64	0.57
Pyramid-Edit	61.44	35.56	83.33	29.98	0.53
TokenFlow	67.78	45.78	68.89	30.23	0.52
VidToMe	67.00	45.33	64.44	28.23	0.21
AnyV2V	65.22	39.11	80.00	30.79	0.97
Ours	71.89	43.56	73.33	31.87	0.65
Dataset V1					
Wan-Edit	73.22	54.56	60.65	36.88	0.37
Pyramid-Edit	65.00	44.56	75.28	32.20	0.36
TokenFlow	71.00	45.78	67.50	33.05	0.32
VidToMe	70.56	46.00	68.61	33.80	0.26
AnyV2V	71.33	43.11	65.56	30.35	0.35
Ours	<u>71.44</u>	<u>49.44</u>	<u>68.89</u>	<u>34.71</u>	0.45

Table 7: Quantitative comparison using our proposed NRVE-Acc metrics alongside inference efficiency for benchmark v1 and v0. We report the overall score, its three components, and the **per-frame inference time**. Underline indicates the second best.

Method	$S_{phy} \uparrow$	$S_{temp} \uparrow$	$S_{instr} \uparrow$	NRVE-Acc \uparrow	Time (s) \downarrow
TokenFlow	70.00	43.33	<u>58.33</u>	31.88	0.32
Pyramid-Edit	56.00	36.67	<u>63.33</u>	25.99	0.36
Wan-Edit	<u>72.67</u>	55.33	<u>58.33</u>	33.87	0.37
VidToMe	<u>76.67</u>	44.00	<u>55.00</u>	31.82	0.26
AnyV2V	68.67	40.00	<u>58.33</u>	28.04	0.35
Ours	75.33	<u>45.33</u>	<u>58.33</u>	<u>32.33</u>	0.45

Table 8: Per-category quantitative comparison on NRVBench (Edit1 ASB) using our proposed NRVE-Acc metric alongside inference efficiency. Scores are reported as percentages ($\times 100$). **Bold** and underline indicate the best and second-best results in each column, respectively.

Method	$S_{phy} \uparrow$	$S_{temp} \uparrow$	$S_{instr} \uparrow$	NRVE-Acc \uparrow	Time (s) \downarrow
TokenFlow	30.82	46.67	60.00	30.82	0.32
Pyramid-Edit	65.33	<u>52.67</u>	66.67	31.88	0.36
Wan-Edit	<u>75.33</u>	57.33	<u>71.67</u>	<u>38.88</u>	0.37
VidToMe	78.00	46.00	63.33	33.26	0.26
AnyV2V	76.67	42.00	46.67	20.59	0.35
Ours	76.67	57.33	73.33	39.49	0.45

Table 9: Per-category quantitative comparison on NRVBench (Edit2 CTS) using our proposed NRVE-Acc metric alongside inference efficiency. Scores are reported as percentages ($\times 100$). **Bold** and underline indicate the best and second-best results in each column, respectively.

Method	$S_{phy} \uparrow$	$S_{temp} \uparrow$	$S_{instr} \uparrow$	NRVE-Acc \uparrow	Time (s) \downarrow
TokenFlow	<u>66.00</u>	<u>52.67</u>	75.00	<u>35.00</u>	0.32
Pyramid-Edit	65.33	42.00	85.00	34.99	0.36
Wan-Edit	67.33	54.67	71.67	36.68	0.37
VidToMe	66.00	48.67	73.33	34.14	0.26
AnyV2V	67.33	47.33	<u>80.00</u>	34.05	0.35
Ours	62.67	49.33	<u>71.67</u>	33.97	0.45

Table 10: Per-category quantitative comparison on NRVBench (Edit3 DSO) using our proposed NRVE-Acc metric alongside inference efficiency. Scores are reported as percentages ($\times 100$). **Bold** and underline indicate the best and second-best results in each column, respectively.

Method	$S_{phy} \uparrow$	$S_{temp} \uparrow$	$S_{instr} \uparrow$	NRVE-Acc \uparrow	Time (s) \downarrow
TokenFlow	73.33	48.67	76.67	35.69	0.32
Pyramid-Edit	<u>72.67</u>	47.33	<u>85.00</u>	37.10	0.36
Wan-Edit	<u>70.67</u>	56.00	78.33	38.42	0.37
VidToMe	78.00	52.67	85.00	39.40	0.26
AnyV2V	37.39	46.67	88.33	<u>37.39</u>	0.35
Ours	69.33	<u>54.00</u>	78.33	<u>37.36</u>	0.45

Table 11: Per-category quantitative comparison on NRVBench (Edit4 GSF) using our proposed NRVE-Acc metric alongside inference efficiency. Scores are reported as percentages ($\times 100$). **Bold** and underline indicate the best and second-best results in each column, respectively.

Method	$S_{phy} \uparrow$	$S_{temp} \uparrow$	$S_{instr} \uparrow$	NRVE-Acc \uparrow	Time (s) \downarrow
TokenFlow	<u>75.33</u>	45.33	<u>73.33</u>	35.19	0.32
Pyramid-Edit	<u>70.00</u>	48.67	83.33	<u>35.23</u>	0.36
Wan-Edit	<u>75.33</u>	<u>51.33</u>	71.67	35.66	0.37
VidToMe	<u>74.67</u>	<u>42.67</u>	73.33	34.44	0.26
AnyV2V	76.00	42.67	71.67	30.30	0.35
Ours	<u>75.33</u>	53.33	65.00	34.28	0.45

Table 12: Per-category quantitative comparison on NRVBench (Edit5 HFF) using our proposed NRVE-Acc metric alongside inference efficiency. Scores are reported as percentages ($\times 100$). **Bold** and underline indicate the best and second-best results in each column, respectively.

Method	$S_{phy} \uparrow$	$S_{temp} \uparrow$	$S_{instr} \uparrow$	NRVE-Acc \uparrow	Time (s) \downarrow
TokenFlow	<u>76.67</u>	38.00	61.67	29.71	0.32
Pyramid-Edit	<u>60.67</u>	40.00	<u>68.33</u>	28.04	0.36
Wan-Edit	78.00	<u>52.67</u>	70.00	37.78	0.37
VidToMe	74.00	42.00	61.67	29.73	0.26
AnyV2V	<u>76.67</u>	40.00	70.00	31.74	0.35
Ours	69.33	<u>37.33</u>	66.67	<u>30.84</u>	0.45

Table 13: Per-category quantitative comparison on NRVBench (Edit6 LFS) using our proposed NRVE-Acc metric alongside inference efficiency. Scores are reported as percentages ($\times 100$). **Bold** and underline indicate the best and second-best results in each column, respectively.

Methods	Structure		Background Preservation				Text Alignment		IQA	Motion	Speed
	Dist.($\times 10^3$) \downarrow	PSNR \uparrow	LPIPS($\times 10^3$) \downarrow	MSE($\times 10^4$) \downarrow	SSIM($\times 10^2$) \uparrow	CLIP-S \uparrow	CLIP-S _{edit} \uparrow	NIQE \downarrow	S.($\times 10^2$) \uparrow	FPS \uparrow	
Edit 1 (NR V1)											
Wan-Edit	18.87	28.41	111.07	19.40	92.48	26.24	22.29	8.05	63.62	/	
Pyramid-Edit	99.61	21.39	154.78	96.60	84.29	26.23	22.29	7.86	56.77	/	
TokenFlow	97.53	21.96	<u>116.07</u>	91.64	76.29	26.24	22.25	8.32	60.43	/	
VidToMe	444.78	10.89	301.27	916.67	58.64	26.82	21.52	7.74	64.50	/	
AnyV2V	393.33	14.33	342.72	520.29	53.76	26.25	22.33	9.38	47.30	/	
TTM	8.22	35.46	43.86	4.39	95.90	26.27	22.34	8.32	65.47	/	

Table 14: Quantitative comparison for Edit 1 on NR V1 benchmark. Best scores in **bold**.

Methods	Structure		Background Preservation				Text Alignment		IQA	Motion	Speed
	Dist.($\times 10^3$) \downarrow	PSNR \uparrow	LPIPS($\times 10^3$) \downarrow	MSE($\times 10^4$) \downarrow	SSIM($\times 10^2$) \uparrow	CLIP-S \uparrow	CLIP-S _{edit} \uparrow	NIQE \downarrow	S.($\times 10^2$) \uparrow	FPS \uparrow	
Edit 2 (NR V1)											
Wan-Edit	7.98	28.24	111.99	20.30	90.65	27.57	24.14	7.80	57.84	/	
Pyramid-Edit	55.28	20.33	176.64	112.48	83.59	27.57	24.14	7.84	54.07	/	
TokenFlow	132.78	20.23	144.10	137.98	67.17	27.58	24.14	7.30	53.04	/	
VidToMe	347.05	11.61	313.83	783.92	51.22	27.29	24.78	7.35	53.13	/	
AnyV2V	336.93	12.94	351.24	706.16	57.01	27.61	24.12	8.61	45.17	/	
TTM	6.56	33.16	62.92	7.77	93.99	27.53	24.20	7.62	58.86	/	

Table 15: Quantitative comparison for Edit 2 on NR V1 benchmark. Best scores in **bold**.

Methods	Structure		Background Preservation				Text Alignment		IQA	Motion	Speed
	Dist.($\times 10^3$) \downarrow	PSNR \uparrow	LPIPS($\times 10^3$) \downarrow	MSE($\times 10^4$) \downarrow	SSIM($\times 10^2$) \uparrow	CLIP-S \uparrow	CLIP-S _{edit} \uparrow	NIQE \downarrow	S.($\times 10^2$) \uparrow	FPS \uparrow	
Edit 3 (NR V1)											
Wan-Edit	21.07	29.32	127.74	15.98	91.38	28.31	26.77	8.67	67.65	/	
Pyramid-Edit	74.32	22.28	153.36	91.08	83.71	28.31	26.77	8.72	56.07	/	
TokenFlow	127.49	21.05	145.05	116.01	77.11	28.34	26.81	3.48	64.39	/	
VidToMe	309.10	12.30	295.12	690.68	63.76	27.64	22.82	9.16	63.23	/	
AnyV2V	246.52	13.74	371.51	743.62	60.55	28.41	26.91	10.00	55.56	/	
TTM	11.28	36.61	48.89	4.11	95.69	28.17	26.62	9.04	66.74	/	

Table 16: Quantitative comparison for Edit 3 on NR V1 benchmark. Best scores in **bold**.

Methods	Structure		Background Preservation				Text Alignment		IQA	Motion	Speed
	Dist.($\times 10^3$) \downarrow	PSNR \uparrow	LPIPS($\times 10^3$) \downarrow	MSE($\times 10^4$) \downarrow	SSIM($\times 10^2$) \uparrow	CLIP-S \uparrow	CLIP-S _{edit} \uparrow	NIQE \downarrow	S.($\times 10^2$) \uparrow	FPS \uparrow	
Edit 4 (NR V1)											
Wan-Edit	15.71	33.68	68.25	6.58	95.51	25.76	24.74	8.01	64.38	/	
Pyramid-Edit	71.59	24.45	82.22	52.12	88.22	25.76	24.74	8.66	57.76	/	
TokenFlow	87.22	22.57	98.33	144.96	81.07	25.77	24.71	0.00	64.26	/	
VidToMe	298.47	13.56	221.78	501.15	72.25	25.73	23.98	9.30	60.13	/	
AnyV2V	322.69	13.61	296.47	732.04	64.21	25.74	24.71	9.94	58.06	/	
TTM	11.32	38.68	32.83	2.24	97.62	25.74	24.80	8.84	62.59	/	

Table 17: Quantitative comparison for Edit 4 on NR V1 benchmark. Best scores in **bold**.

Methods	Structure		Background Preservation				Text Alignment		IQA	Motion	Speed
	Dist.($\times 10^3$) \downarrow	PSNR \uparrow	LPIPS($\times 10^3$) \downarrow	MSE($\times 10^4$) \downarrow	SSIM($\times 10^2$) \uparrow	CLIP-S \uparrow	CLIP-S _{edit} \uparrow	NIQE \downarrow	S.($\times 10^2$) \uparrow	FPS \uparrow	
Edit 5 (NR V1)											
Wan-Edit	10.07	28.57	138.81	21.44	90.95	25.82	23.10	8.20	60.82	/	
Pyramid-Edit	55.22	20.00	176.44	128.93	83.98	25.82	23.10	7.70	52.36	/	
TokenFlow	83.39	20.31	157.18	111.18	75.12	25.82	23.11	0.00	57.63	/	
VidToMe	303.81	11.44	345.55	859.00	58.90	25.27	22.09	7.51	57.28	/	
AnyV2V	278.45	14.84	364.85	494.66	66.39	25.85	23.11	8.91	45.93	/	
TTM	6.69	34.90	49.89	6.46	95.10	25.79	23.00	7.64	60.75	/	

Table 18: Quantitative comparison for Edit 5 on NR V1 benchmark. Best scores in **bold**.

Methods	Structure		Background Preservation				Text Alignment		IQA	Motion	Speed
	Dist.($\times 10^3$) \downarrow	PSNR \uparrow	LPIPS($\times 10^3$) \downarrow	MSE($\times 10^4$) \downarrow	SSIM($\times 10^2$) \uparrow	CLIP-S \uparrow	CLIP-S _{edit} \uparrow	NIQE \downarrow	S.($\times 10^2$) \uparrow	FPS \uparrow	
Edit 6 (NR V1)											
Wan-Edit	32.27	27.99	113.68	20.38	91.94	26.26	21.95	8.93	49.58	/	
Pyramid-Edit	143.76	21.94	140.99	90.23	83.20	26.26	21.95	8.81	46.32	/	
TokenFlow	155.19	20.47	145.11	107.63	75.01	26.25	21.95	0.00	51.22	/	
VidToMe	486.37	11.00	326.30	918.97	53.92	26.87	22.17	8.96	48.26	/	
AnyV2V	398.12	13.51	396.83	682.74	48.94	26.31	21.91	9.95	42.83	/	
TTM	8.09	35.94	48.93	3.46	96.02	26.23	21.94	9.15	51.25	/	

Table 19: Quantitative comparison for Edit 6 on NR V1 benchmark. Best scores in **bold**.

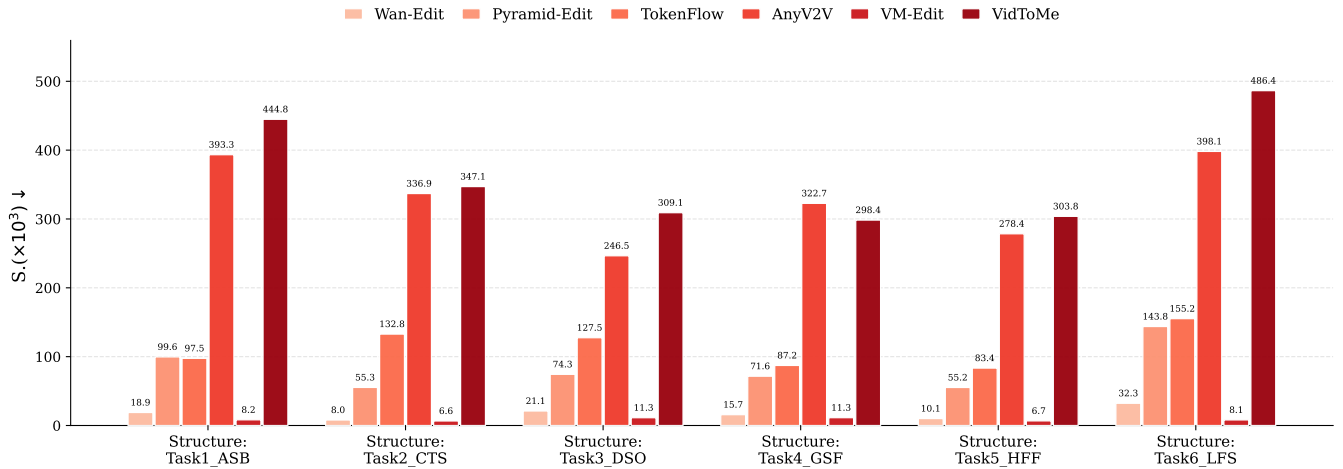


Figure 9: The Structure Distance for the six models.

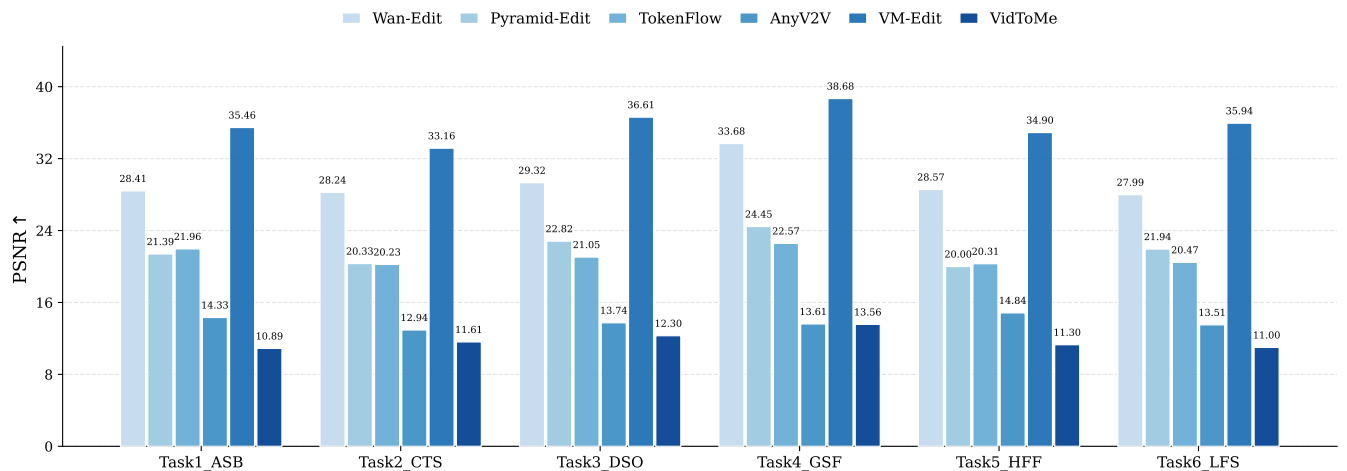


Figure 10: The PSNR background preservation for the six models

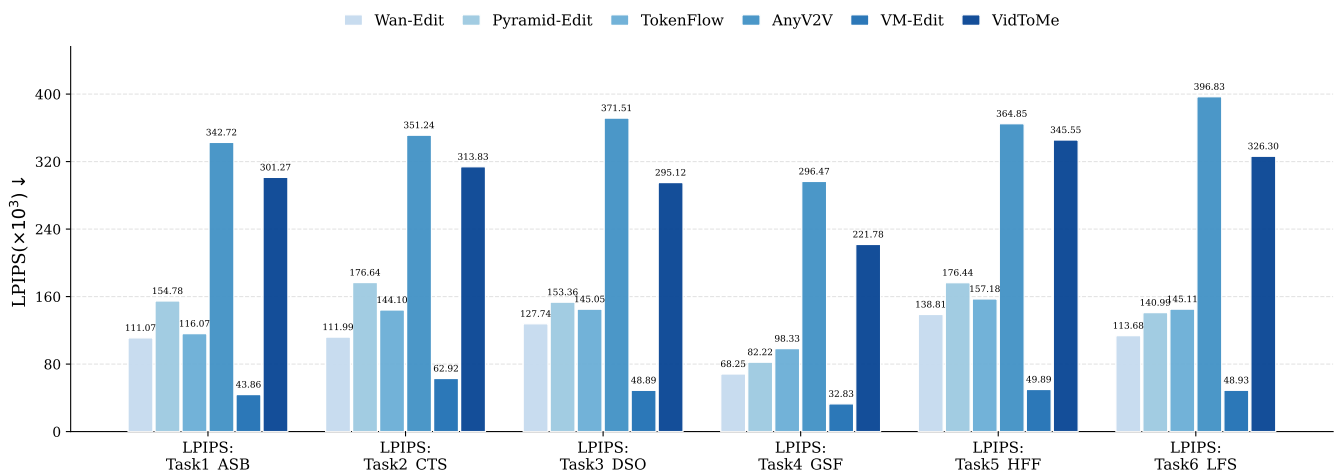


Figure 11: The LPIPS background preservation for the six models

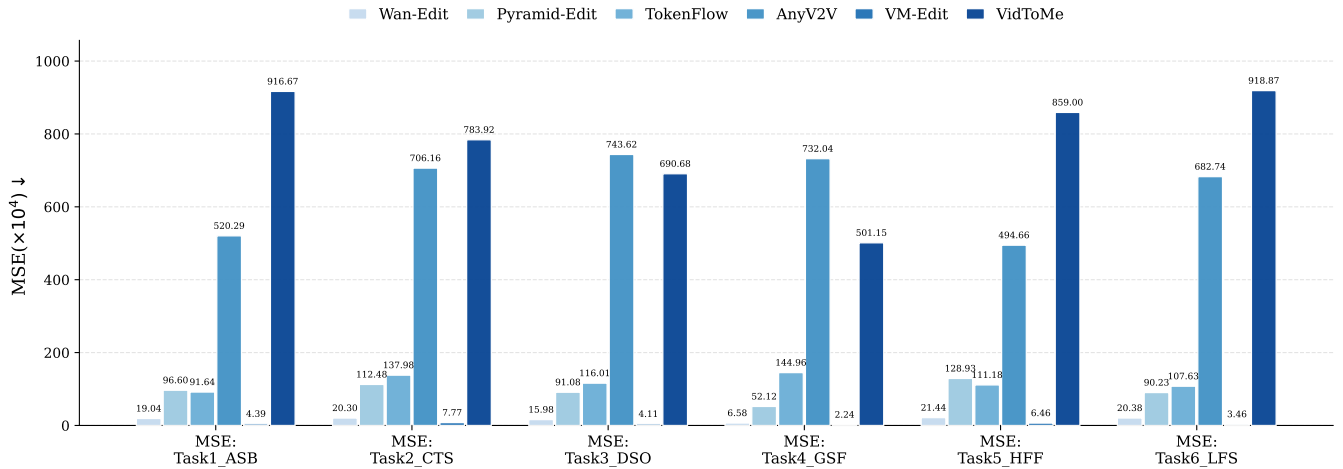


Figure 12: The MSE background preservation for the six models

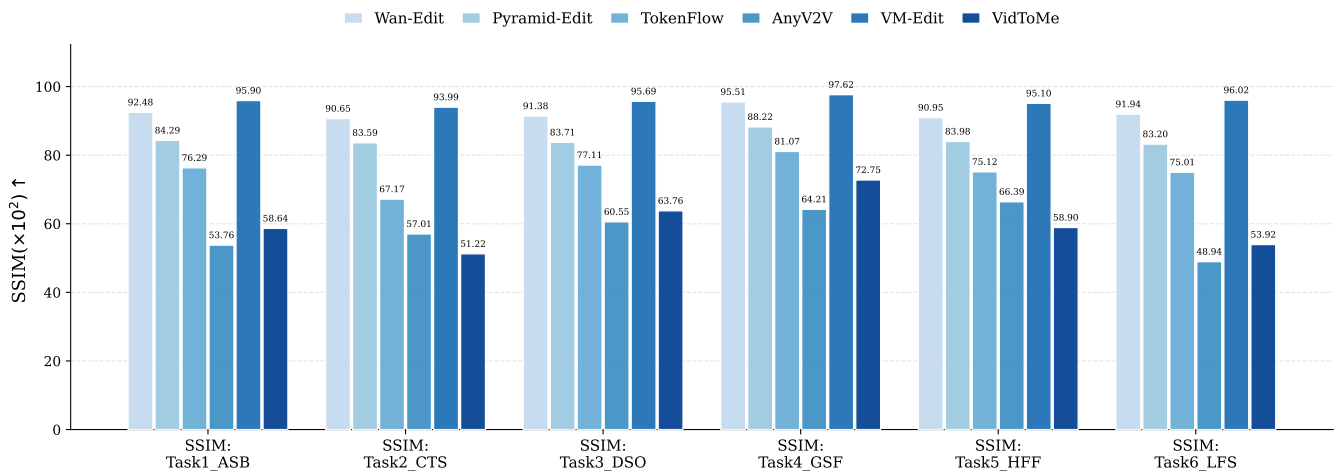


Figure 13: The SSIM background preservation for the six models

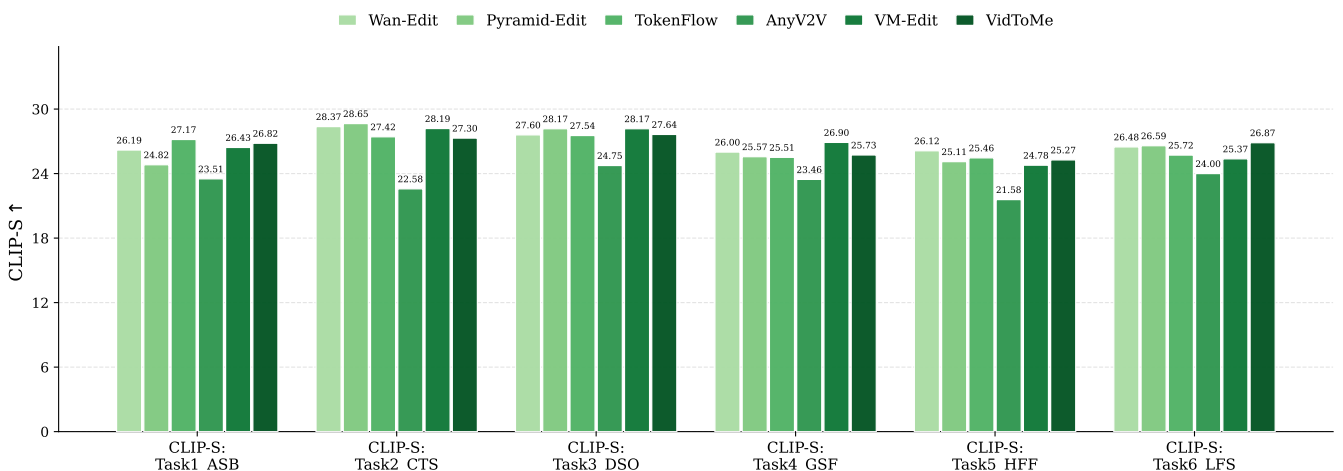


Figure 14: The text alignment CLIP-S data for the six models

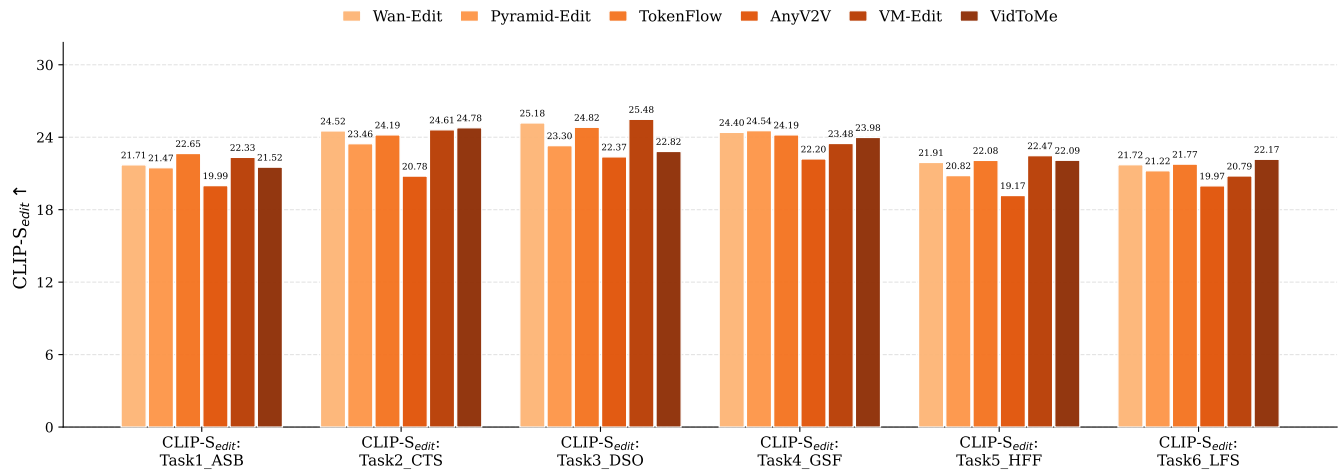


Figure 15: The text alignment CLIP-S-edit data for the six models

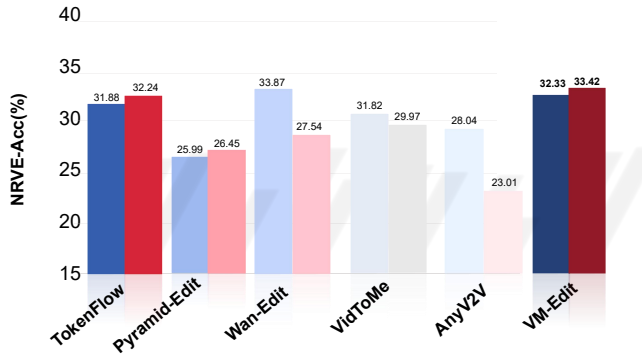


Figure 16: NRVE-Acc results(Left) and human evaluation(Right) on ASB.

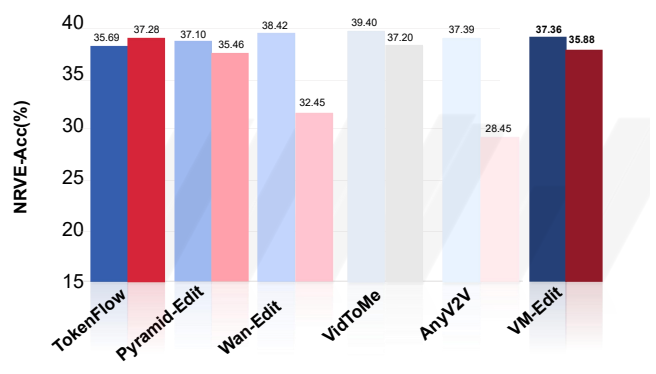


Figure 19: NRVE-Acc results(Left) and human evaluation(Right) on GSF.

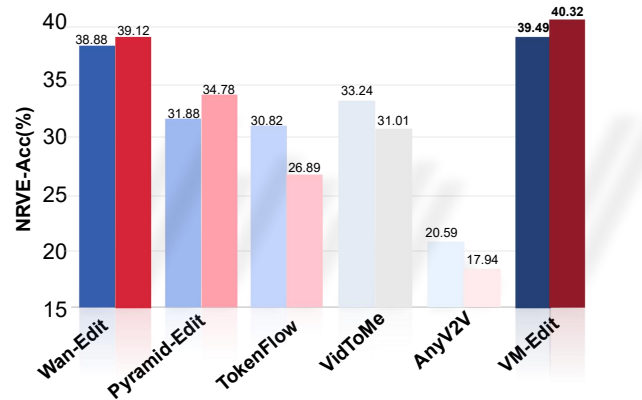


Figure 17: NRVE-Acc results(Left) and human evaluation(Right) on CTS

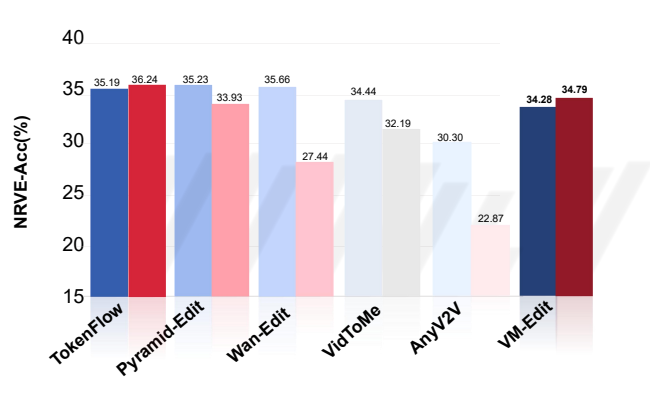


Figure 20: NRVE-Acc results(Left) and human evaluation(Right) on HFF.

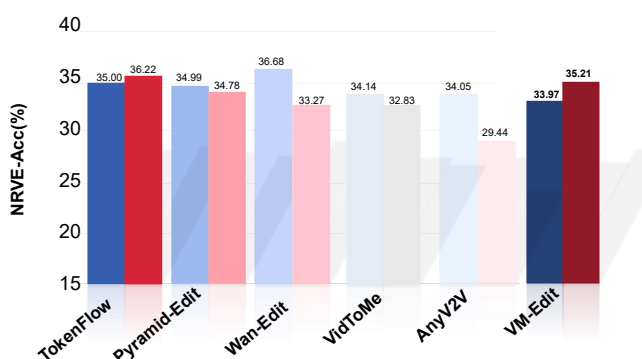


Figure 18: NRVE-Acc results(Left) and human evaluation(Right) on DSO.

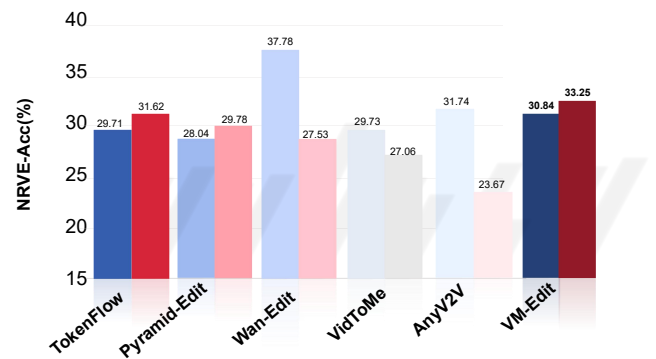


Figure 21: NRVE-Acc results(Left) and human evaluation(Right) on LFS.